Supplementary Information

Polar Alcohol Guest Molecules Regulate the Stacking Modes of 2-D MOF Nanosheets

Yue Cheng[+], Wen-Qi Tang[+], Lu-Ting Geng, Ming Xu, Jian-Ping Zhu, Sha-Sha Meng, and Zhi-Yuan Gu*

Jiangsu Key Laboratory of Biofunctional Materials, Jiangsu Collaborative Innovation Center of Biomedical Functional Materials, Jiangsu Key Laboratory of New Power Batteries, College of Chemistry and Materials Science, Nanjing Normal University, Nanjing 210023, China, e-mail: guzhiyuan@njnu.edu.cn

Table of Contents

Section S1: Chemicals and Instrumentation

All compounds were purchased from commercial sources. Zirconium chloride ($ZrCl_4$), 1,3,5-(4-carboxylphenyl)-benzene (H_3BTB), 1,3,5-(4-carboxylphenyl)-nitrogen (H_3TCA) and 4,4',4''- (1,3,5-triazine-2,4,6-triyl) tribenzoic acid (H_3TATB) were purchased from J&K Scientific Ltd. (Beijing, China) and Henghua Sci. & Tec. Co., Ltd. (Jinan, China), respectively. methyl alcohol (MeOH), ethyl alcohol (EtOH), propyl alcohol (PrOH), formic acid (FA), xylene isomers and ethylbenzene, chlorotoluene isomers, dichlorotoluene isomers, and ethyl toluene isomers were bought from Aladdin Co. Ltd (Shanghai, China). N,N-dimethylformmide (DMF) and ethanol were purchased from Sinopharm Chemical Reagent Co. Ltd (Shanghai, China). DMF were immersed in molecular sieve for 24 h to remove the water. Ultrapure water (18 MΩ·cm) from an ELGA purification system (Veolia Water Solutions &Technologies, UK) was used throughout this work.

Powder X-ray diffraction (PXRD) patterns were obtained from Bruker Powder Diffractometer ECO with CuKα radiation (1.54056 Å). The transmission electron microscopy (TEM) images were collected on JEOL JEM-2100F. The scanning electron microscope (SEM) images were collected on a JSM-7600 scanning electron microscope (JEOL Ltd.). The high-resolution transmission electron microscopy (HRTEM) images were obtained from JEM-2100F, 200 kV, JEOL, Japan. The high angel annular dark field (HAADF) images of the materials were recorded on an ARM-200CF TEM (JEOL, Tokyo, Japan) operated at 200 keV and equipped with double spherical aberration (Cs) correctors. Thermogravimetric analysis (TGA) was collected on a Perkin-Elmer Pyris Diamond 1 TGA analyzer. Proton nuclear magnetic resonance (HNMR) was recorded on a Bruker AN-400 MHz instrument. Atomic force microscopy (AFM) measurements were performed in tapping mode (5100 N, HITACHI). Thermogravimetric analysis (TGA) was collected on a Perkin-Elmer Pyris Diamond 1 TGA analyzer. All of the separations were performed on an Agilent 7890B gas chromatographic system with a flame ionization detector (FID). Data acquisition and processing were controlled by Chem Station software. Nitrogen (99.999%, Air Liquide, France) was employed as the

carrier gas. The inlet temperature of the GC was set to 250 ºC, while the temperature of FID was set to 300 ºC. A 2 μL analyte was introduced to a 20 mL gastight-sealed glass vial and homogenized at 100 ºC before the injection for gas chromatographic separation.

Section S2: Synthesis of Zr-BTB, Zr-TCA and Zr-TATB

Synthesis of 2-D Zr-BTB-MeOH

2-D Zr-BTB nanosheets were synthesized according to the previous report with a minor change.[1] Briefly, H_3BTB (12.50 mg) and $ZrCl_4$ (10.12 mg) were dissolved in DMF (5 mL) in a 20 mL pyrex vial. FA (1.313 g) and H_2O (60 μL) added to the mixture of DMF. The vial was sealed and heated at 120 ^oC for 48 h in the oven, then cooled to room temperature after the reaction. The 2-D Zr-BTB-MeOH were collected by centrifugation and washed with DMF and methanol three times respectively. Then, the material was dried in a fume hood.

Synthesis of 2-D Zr-BTB-EtOH

2-D Zr-BTB nanosheets were synthesized according to the previous report with a minor change.[1] Briefly, H_3BTB (12.50 mg) and $ZrCl_4$ (10.12 mg) were dissolved in DMF (5 mL) in a 20 mL pyrex vial. FA (1.313 g) and H_2O (60 μL) added to the mixture of DMF. The vial was sealed and heated at 120 ^oC for 48 h in the oven, then cooled to room temperature after the reaction. The 2-D Zr-BTB-EtOH were collected by centrifugation and washed with DMF and ethanol three times respectively. Then, the material was dried in a fume hood.

Synthesis of 2-D Zr-BTB-PrOH

2-D Zr-BTB nanosheets were synthesized according to previous report with a minor change.[1] Briefly, H_3BTB (12.50 mg) and $ZrCl_4$ (10.12 mg) were dissolved in DMF (5 mL) in a 20 mL pyrex vial. FA (1.313 g) and H_2O (60 μL) added to the mixture of DMF. The vial was sealed and heated at 120 ^oC for 48 h in the oven, then cooled to room temperature after the reaction. The 2-D Zr-BTB-PrOH were collected by centrifugation and washed with DMF and propyl alcohol three times respectively. Then, the material was dried in a fume hood.

Synthesis of 2-D Zr-TCA-MeOH

2-D Zr-TCA nanosheets were synthesized according to previous report with a minor change.[1] Briefly, H_3TCA (10.76 mg) and $ZrCl_4$ (10.12 mg) were dissolved in DMF (5 mL) in a 20 mL pyrex vial. FA (1.113 g) and H_2O (60 μL) added to the mixture of DMF.

The vial was sealed and heated at 120 °C for 48 h in the oven, then cooled to room temperature after the reaction. The 2-D Zr-TCA-MeOH were collected by centrifugation and washed with DMF and methanol three times respectively. Then, the material was dried in a fume hood.

Synthesis of 2-D Zr-TCA-EtOH

2-D Zr-TCA nanosheets were synthesized according to the previous report with a minor change.[1] Briefly, H_3TCA (12.50 mg) and $ZrCl_4$ (10.12 mg) were dissolved in DMF (5 mL) in a 20 mL pyrex vial. FA (1.113 g) and H_2O (60 μL) added to the mixture of DMF. The vial was sealed and heated at 120 °C for 48 h in the oven, then cooled to room temperature after the reaction. The 2-D Zr-TCA-EtOH were collected by centrifugation and washed with DMF and ethanol three times respectively. Then, the material was dried in a fume hood.

Synthesis of 2-D Zr-TCA-PrOH

2-D Zr-TCA nanosheets were synthesized according to the previous report with a minor change.[1] Briefly, H_3TCA (12.50 mg) and $ZrCl_4$ (10.12 mg) were dissolved in DMF (5 mL) in a 20 mL pyrex vial. FA (1.113 g) and H_2O (60 μL) added to the mixture of DMF. The vial was sealed and heated at 120 °C for 48 h in the oven, then cooled to room temperature after the reaction. The 2-D Zr-TCA-PrOH were collected by centrifugation and washed with DMF and propyl alcohol three times respectively. Then, the material was dried in a fume hood.

Synthesis of 2-D Zr-TATB-EtOH

2-D Zr-TATB nanosheets were synthesized according to the previous report with a minor change.[1] Briefly, H_3TATB (12.5 mg) and $ZrCl_4$ (10.12 mg) were dissolved in DMF (5 mL) in a 20 mL pyrex vial. FA (700 μL) and H_2O (240 μL) added to the mixture of DMF. The vial was sealed and heated at 120 °C for 24 h in the oven, then cooled to room temperature after the reaction. The 2-D Zr-TATB-EtOH were collected by centrifugation and washed with DMF and ethanol three times respectively. Then, the material was dried in a fume hood.

Section S3: Characterization of Zr-BTB

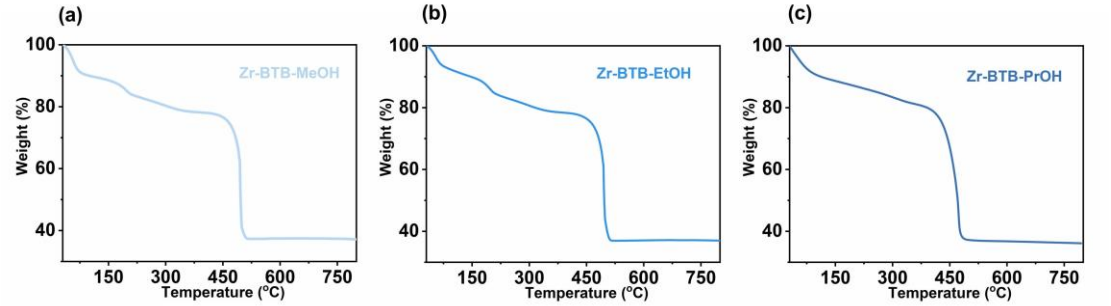

Figure S1. TGA curves of 2-D Zr-BTB. TGA curves of (a) Zr-BTB-MeOH, (b) Zr-BTB-EtOH, (c) Zr-BTB-PrOH.

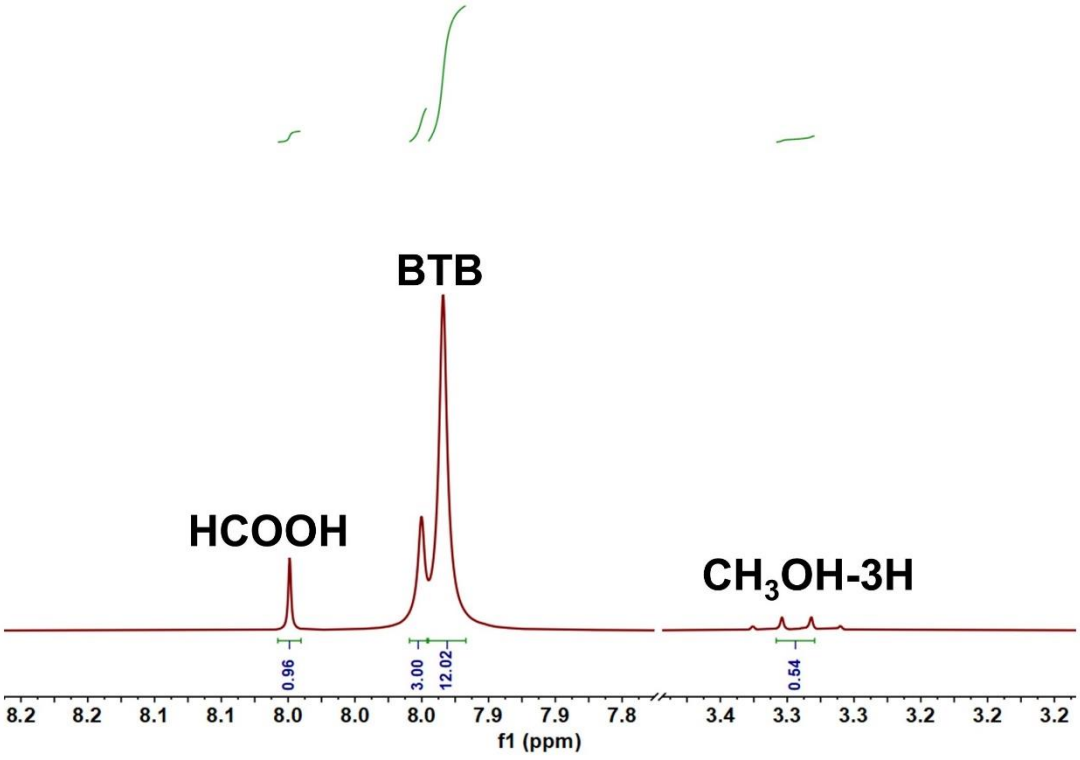

Figure S2. HNMR of 2-D Zr-BTB-MeOH nanosheets. The molar ratio of n(CH_3OH): n(BTB)=0.21:1 was collected from the peak integration. The nanosheet sample (around 4 mg) was digested in d_6-DMSO-D_2SO_4 (v:v=1:1,100 μL), and then in d_6-DMSO (600 μL) before HNMR measurement.

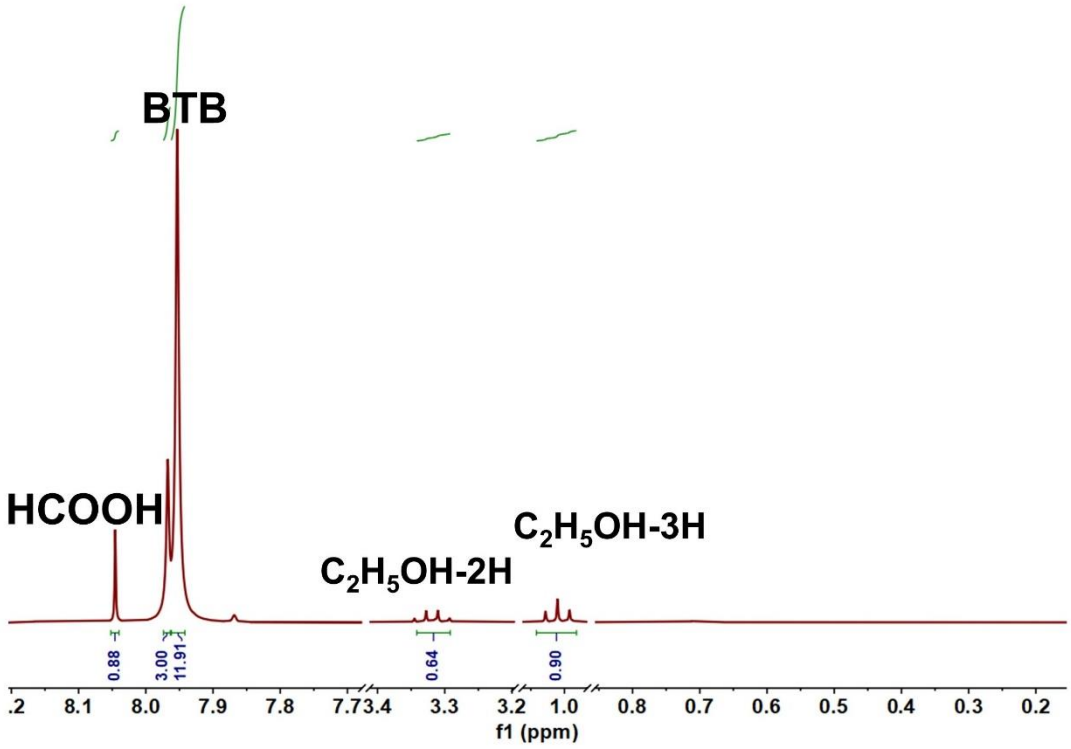

Figure S3. HNMR of 2-D Zr-BTB-EtOH nanosheets. The molar ratio of n(C_2H_5OH): n(BTB)=0.32:1 was collected from the peak integration. The nanosheet sample (around 4 mg) was digested in d_6-DMSO-D_2SO_4 (v:v=1:1,100 μL), and then in d_6-DMSO (600 μL) before HNMR measurement.

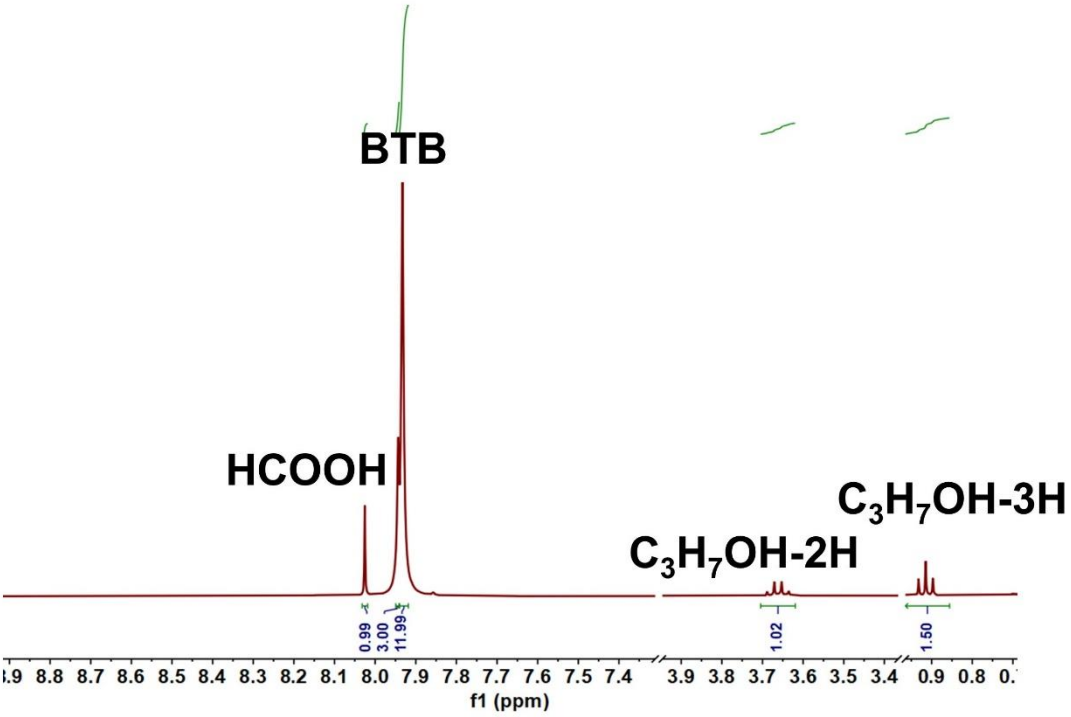

Figure S4. HNMR of 2-D Zr-BTB-PrOH nanosheets. The molar ratio of n(C_3H_7OH): n(BTB)=0.51: 1 was collected from the peak integration. The nanosheet sample (around 4 mg) was digested in d_6-DMSO-D_2SO_4 (v:v=1:1,100 μL), and then in d_6-DMSO (600 μL) before HNMR measurement.

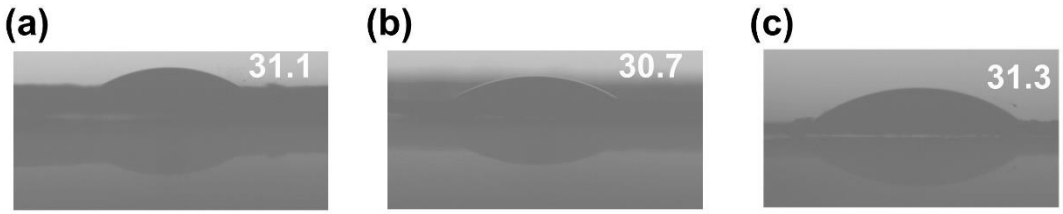

Figure S5. The water contact angle photographs of 2-D Zr-BTB-MeOH nanosheets. (a-c) The water contact angle photographs were the data of the three measurements respectively. Sample preparation: the nanosheets were pressed into smooth, flat pieces.

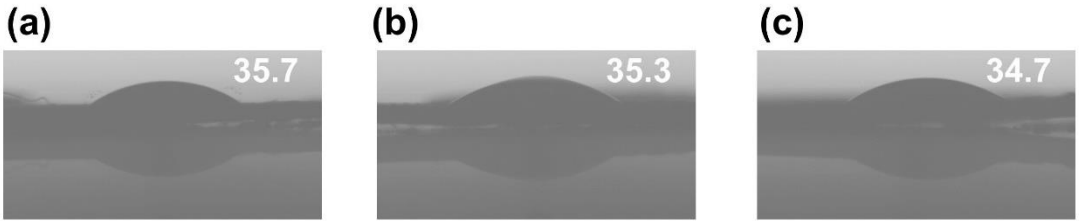

Figure S6. The water contact angle photographs of 2-D Zr-BTB-EtOH nanosheets. The water contact angle photographs were the data of the three measurements respectively. Sample preparation: the nanosheets were pressed into smooth, flat pieces.

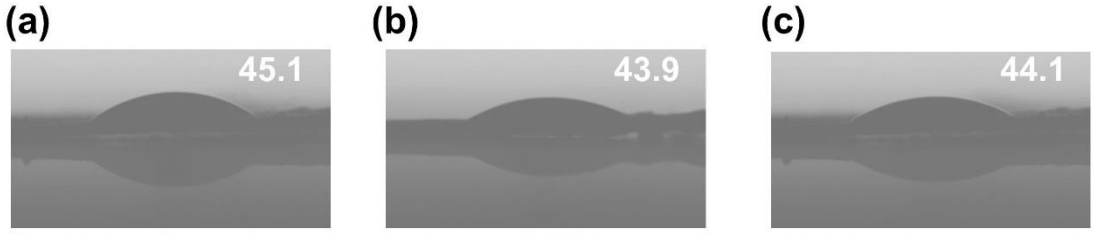

Figure S7. The water contact angle photographs of 2-D Zr-BTB-PrOH nanosheets. The water contact angle photographs were the data of the three measurements respectively. Sample preparation: the nanosheets were pressed into smooth, flat pieces.

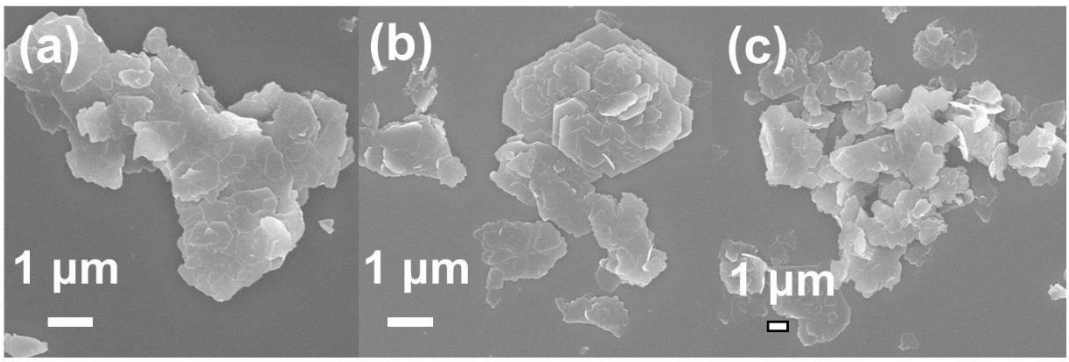

Figure S8. SEM images of (a) Zr-BTB-MeOH, (b) Zr-BTB-EtOH and (c) Zr-BTB-PrOH. The nanosheet samples were ultrasonic in methyl alcohol, ethanol and propanol solvent for 1 h before TEM measurement, respectively.

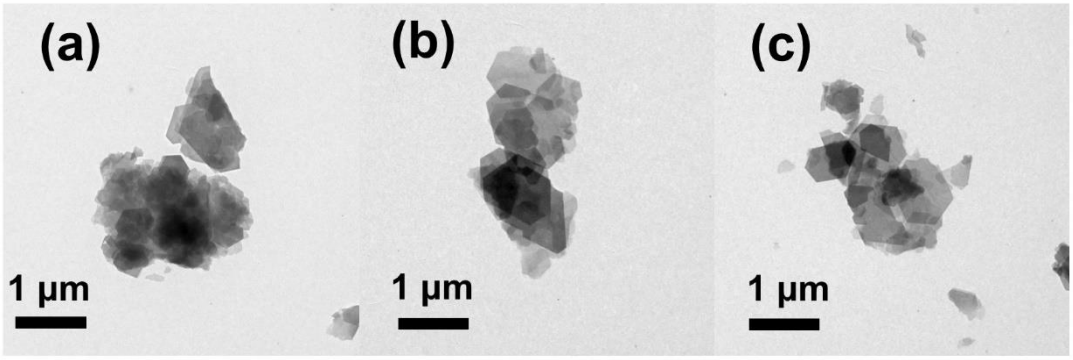

Figure S9. TEM images of (a) Zr-TCA-MeOH, (b) Zr-TCA-EtOH and (c) Zr-TCA-PrOH. The nanosheet samples were ultrasonic in methyl alcohol, ethanol and propanol solvent for 1h before TEM measurement respectively.

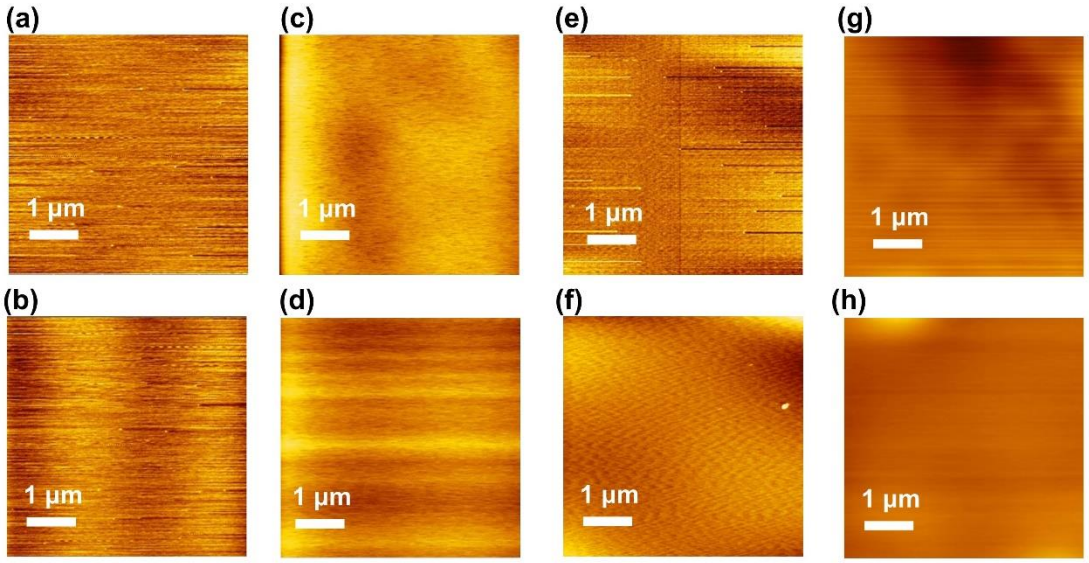

Figure S10. AFM images of (a-b) blank mica, (c-d) blank mica substrates after deposition of pure methanol, (e-f) blank mica substrates after deposition of pure ethanol, and (g-h) blank mica substrates after deposition of pure propyl alcohol. Images characteristic of the ultrathin 2-D nanosheets were not observed.

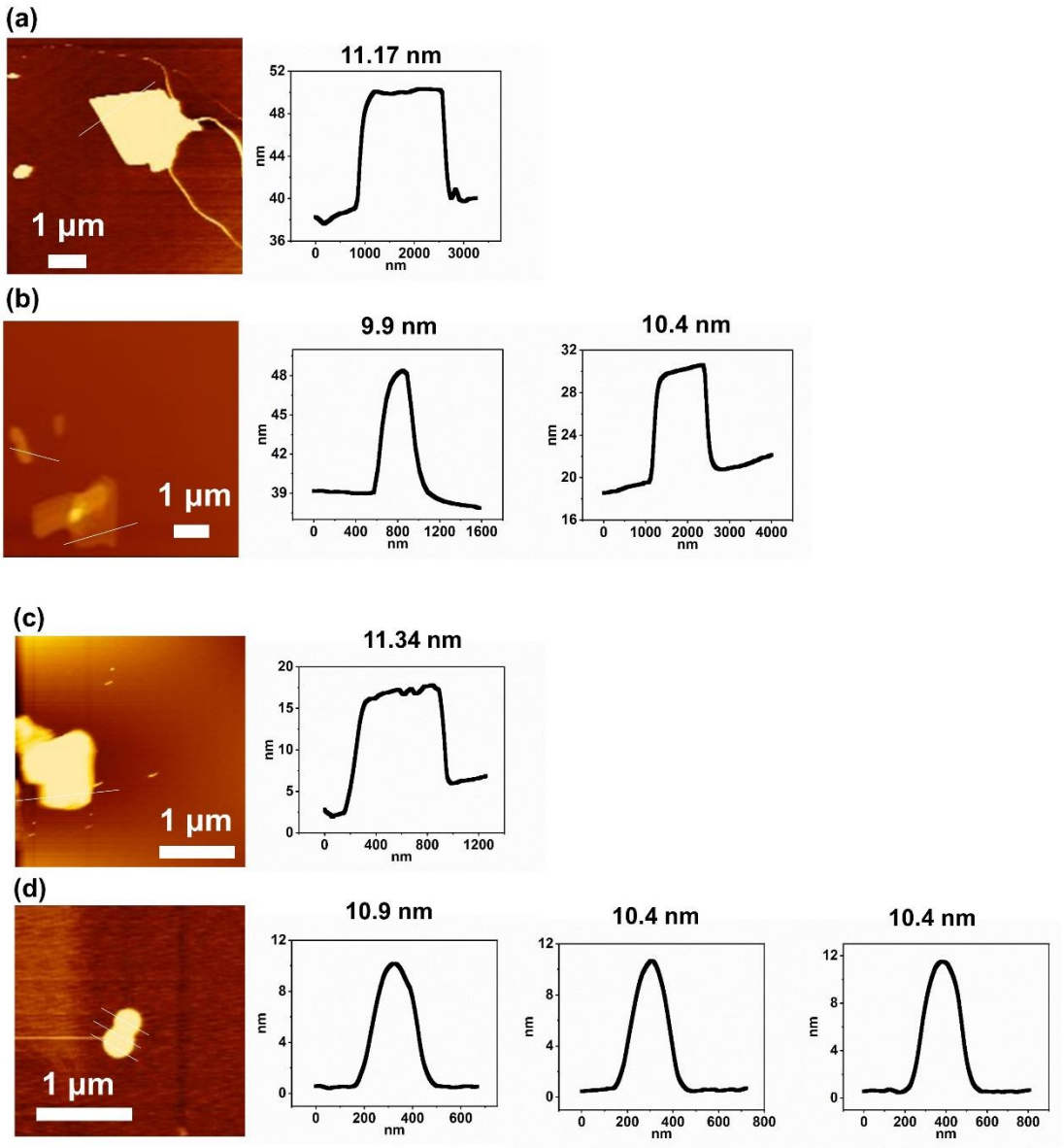

Figure S11. Atomic force microscope (AFM) measurements of 2-D Zr-BTB-MeOH nanosheets. Sample preparation: The Zr-BTB-MeOH nanosheets were dispersed into methanol solvent and then dripped onto blank mica substrates.

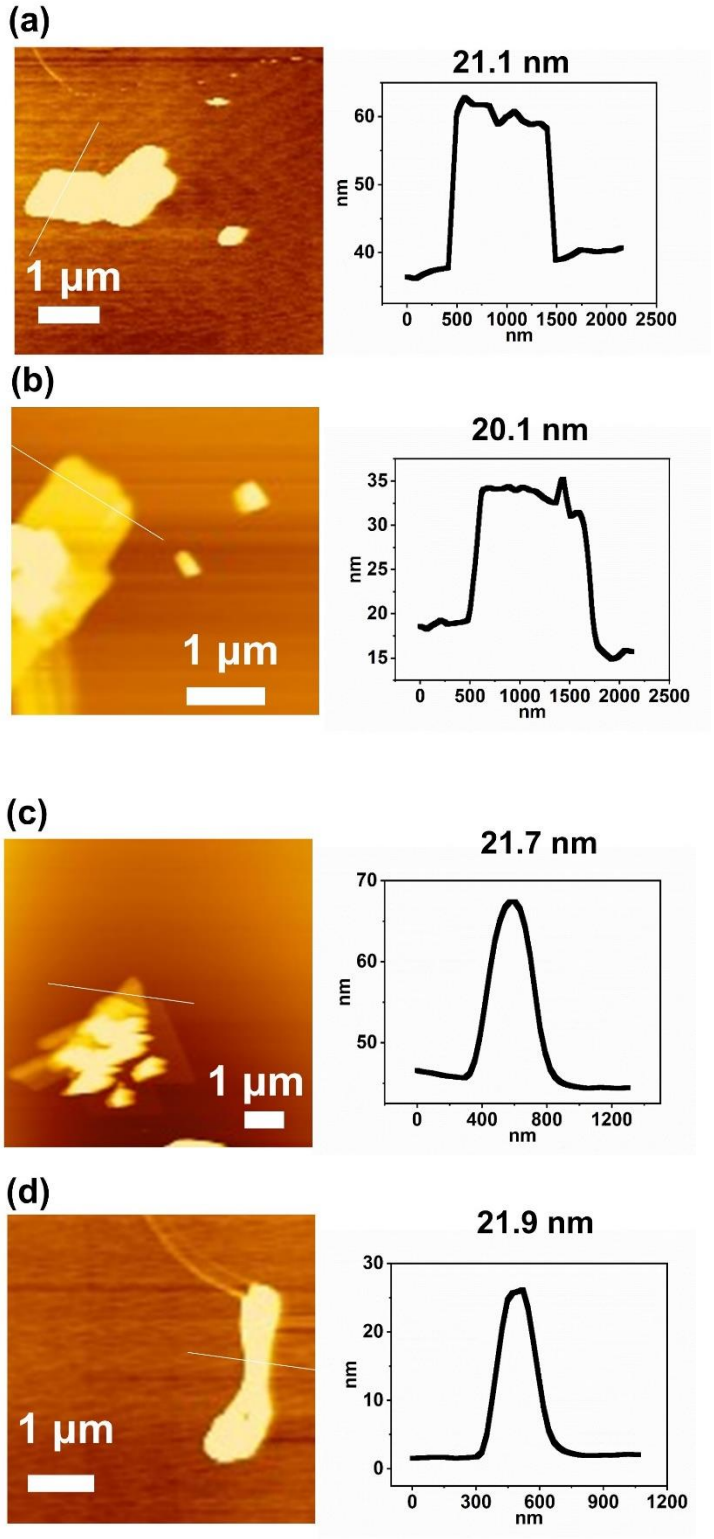

Figure S12. Atomic force microscope (AFM) measurements of 2-D Zr-BTB-EtOH nanosheets. Sample preparation: The Zr-BTB-EtOH nanosheets were dispersed into ethanol solvent and then dripped onto blank mica substrates.

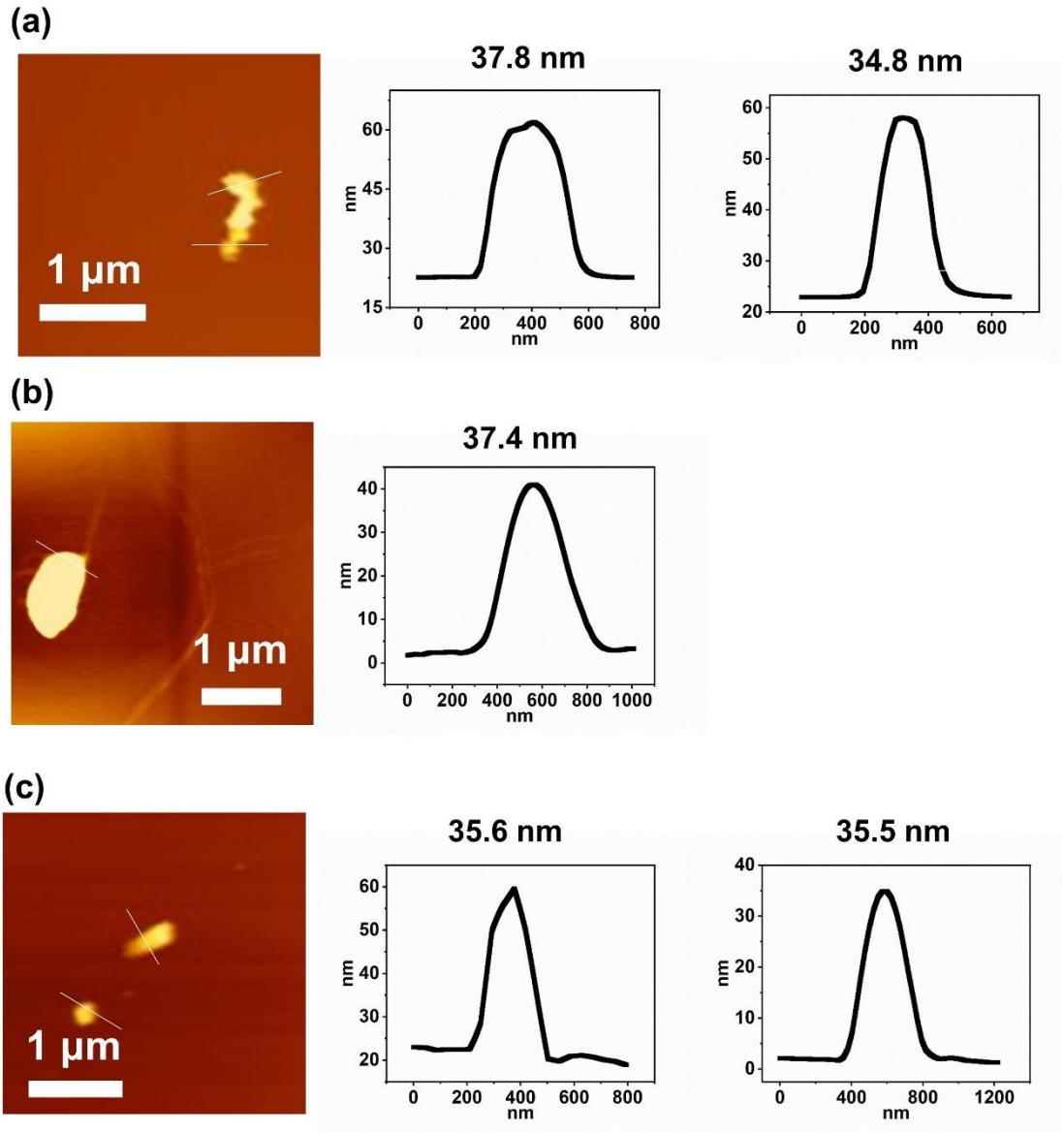

Figure S13. Atomic force microscope (AFM) measurements of 2-D Zr-BTB-PrOH nanosheets. Sample preparation: The Zr-BTB-PrOH nanosheets were dispersed into propanol solvent and then dripped onto blank mica substrates.

Section S4: The statistical methods for angle distribution

To accurately quantify the distribution of stacking angles in nanosheets, we divided each HAADF-STEM image into identical grids (e.g. 50 nm × 50 nm) and measured the angles through corresponding FFT images. An example was showed to explain the statistical methods. Firstly, we divided 16 small grids (with each grid about 50 nm × 50 nm) in the HAADF-STEM images based on the scale bar. After that, the angles were measured through FFT images with the corresponding HAADF-STEM image using Digital Micrograph software, respectively. The 16 angles were measured in the picture. All angles from different grids in different HAADF images were summarized to generate the angle distribution, such as Zr-BTB-MeOH in Figure 2m with the data from n=922 grids. The statistical analysis of all HAADF-STEM images was performed with this method.

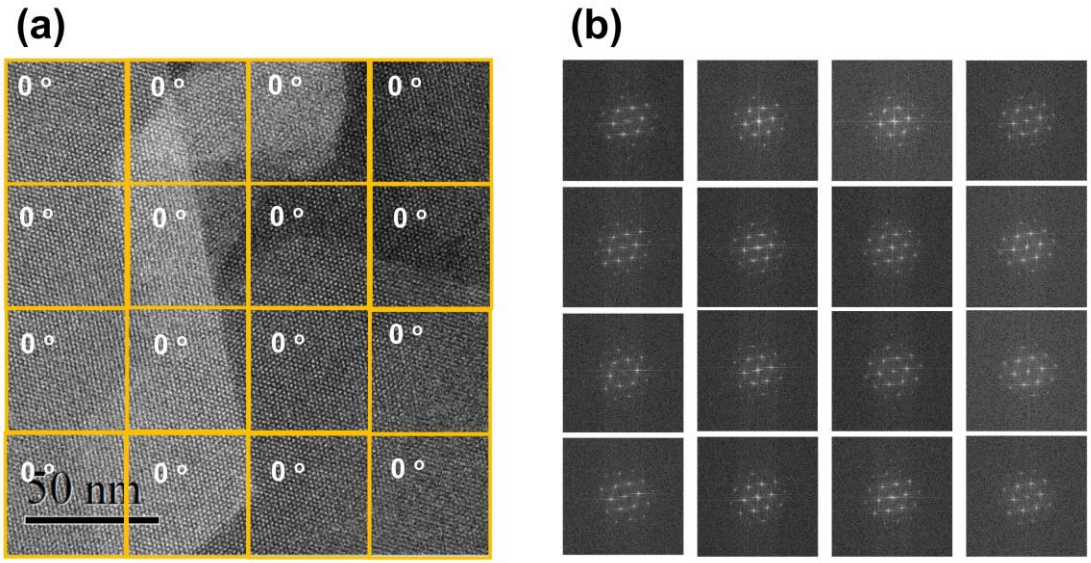

Figure S14. The example of accurately quantifying the distribution of stacking angles in Zr-BTB-MeOH nanosheets. We divided each HAADF-STEM image into identical grids and measured the angles through corresponding FFT images. (a) The HAADF image with 16 grids. (b) Their corresponding FFT images.

Section S5: Computational Simulation of Zr-BTB

All calculations were carried out with the CP2K package (version 7.1) in the framework of the density functional theory,[2] based on the hybrid Gaussian and plan-wave scheme.[3] Molecular orbitals of the valence electrons were expanded into DZVP-MOLOPT-SR-GTH basis sets,[4] while atomic core electrons are described through Goedecker-Teter-Hutter (GTH) pseudopotentials.[5] A plane-wave density cutoff of 500 Ry was adopted. The long - range van der Waals interaction is described by the DFT-D3 approach.[6] All the structures fully relaxed by CP2K with BFGS scheme, and the force convergence criterion was set to $4.5 * 10^{-4}$ hartree/bhor. To study the charge transfer between Zr-BTB nanosheets and methanol molecule, Bader charge analysis was carried out to analyze the electron structure of different adsorption sites.

Section S6: SEM Images of Zr-BTB Coated Columns and Gas Chromatogram for the Separation of Different Analytes.

Capillary pretreatment:

A fused silica capillary (15 m long × 0.25 mm i.d., Yongnian Optic Fiber Plant, Hebei, China) was pre-treated according to the following recipe before dynamic coating with the materials: the capillary was washed sequentially with 1 mol/L NaOH for 2 h, ultrapure water for 30 min, 0.1 mol/L HCl for 2 h, ultrapure water again until the outflow reached pH=7.0, and finally methanol for 30 min. After the above process, the capillary was modified with 3-aminopropyltriethoxysilane (APTES) to provide the amino groups to enhance the interactions with nanosheets on the inner wall of the capillary column.[7] The pretreated capillary was filled with a methanol solution of APTES (50%, v/v), and incubated in a 40 ^{o}C water bath overnight with both ends of the capillary sealed. The APTES-modified capillary was rinsed with methanol to flush out the residuals and dried with a stream of nitrogen at 120 ^{o}C.

Coating the materials:

Different materials were coated onto the pretreated capillary column by a simple dynamic coating method as follows: 1 mL (2 mg/mL) methanol suspension of each material was first filled into the capillary column and then pushed through the column at a velocity of 30 cm/min to leave a wet coating layer on the inner wall of the capillary column. After coating, the capillary column was settled for conditioning under nitrogen for 2 h to remove the solvent. Further conditioning of the capillary column was carried out using a temperature program: maintain 30 ^{o}C for 30 min, then ramp to 250 ^{o}C at a rate of 2 ^{o}C/min and keep 250 ^{o}C for 180 min. The temperature program was repeated 3 times.

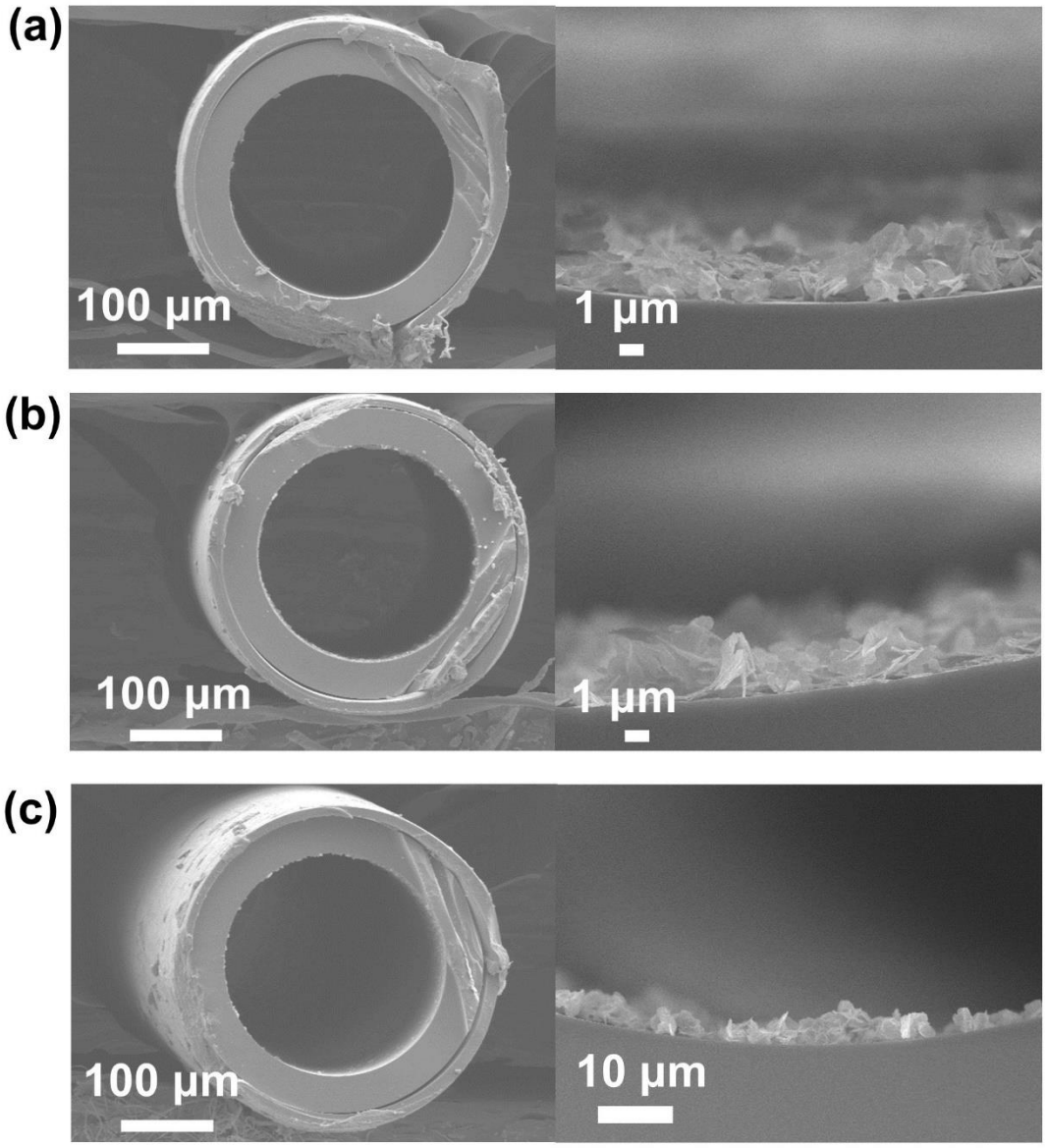

Figure S15. SEM images of 2-D Zr-BTB capillary columns with a cross-sectional view. (a) 2-D Zr-BTB-MeOH capillary columns, (b) 2-D Zr-BTB-EtOH capillary columns, and (c) 2-D Zr-BTB-PrOH capillary columns.

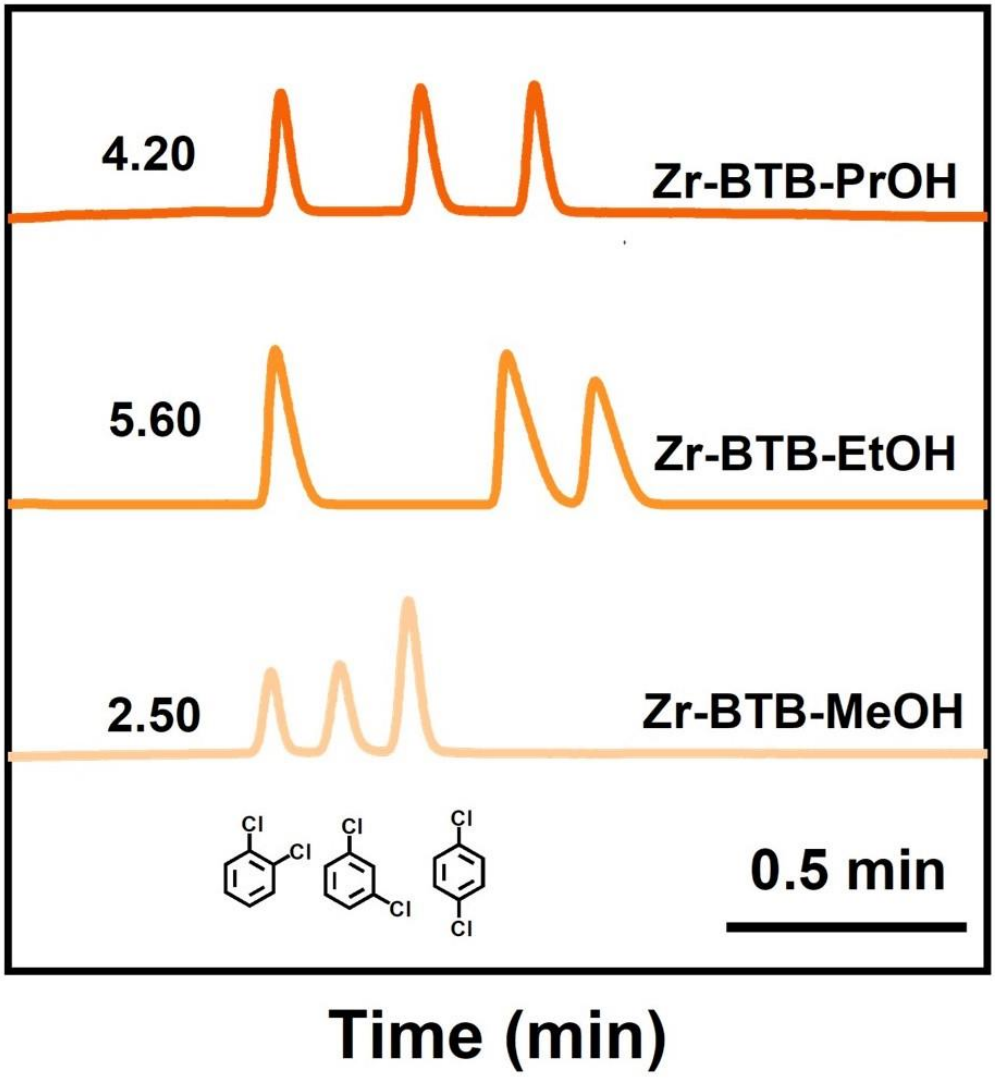

Figure S16. Gas chromatograms of 2-D Zr-BTB nanosheets for the separation of dichlorobenzene.

Section S7: Calculation of Thermodynamic Parameters

The adsorption enthalpy (ΔH) was calculated via the van't Hoff equation:

$$lnk' = -\frac{\Delta H}{RT} + \frac{\Delta S}{R} + ln\emptyset$$

Where *k'* is the retention factor, R is the gas constant, T is the absolute temperature, and *Ø* is the phase ratio (the ratio of the volume of the stationary phase (V_s) to that of the mobile phase (V_m)). To obtain *Ø*, V_s was calculated from the film thickness of nanosheets coated capillary column, while V_m was calculated from the column internal volume subtract the *Vs*.

The *k'* was calculated according to the next equation:

$$k' = \frac{t - t_0}{t_0}$$

Where *t* is the retention time of the analyte, and t_0 is the retention time of an unretained compound on the column.

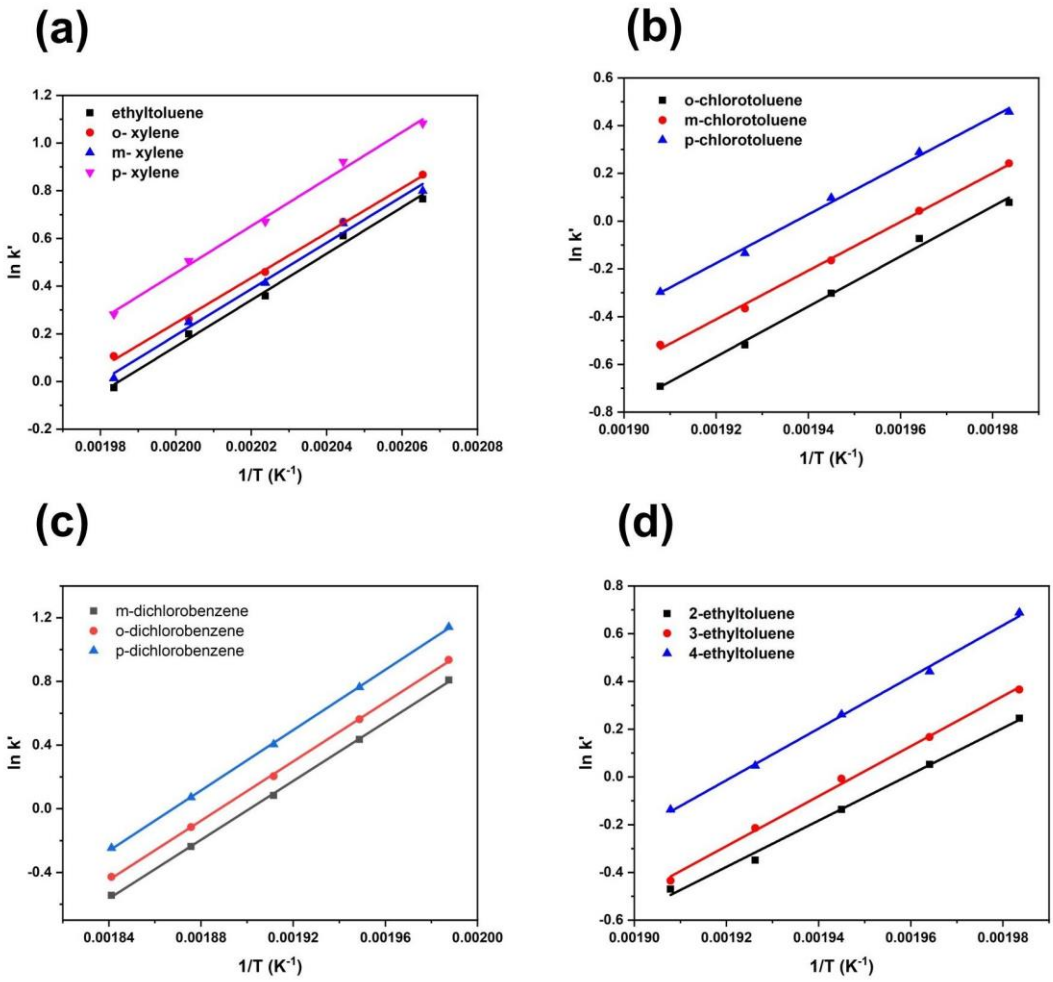

Figure S17. van't Hoff plots for (a) the xylene isomers and ethylbenzene, (b) chlorotoluene isomers, (c) dichlorotoluene isomers, and (d) and ethyl toluene isomers on the Zr-BTB-MeOH capillary column.

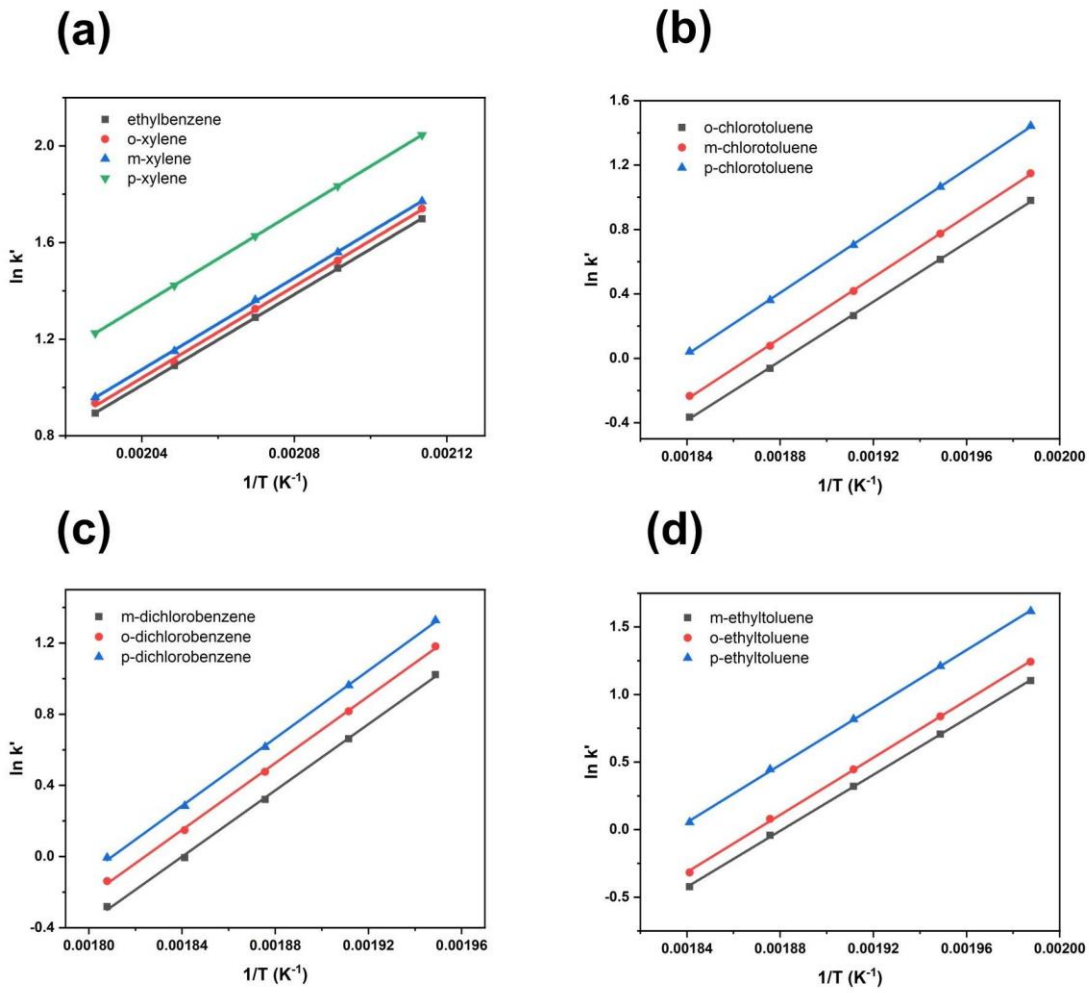

Figure S18. van't Hoff plots for (a) the xylene isomers and ethylbenzene, (b) chlorotoluene isomers, (c) dichlorotoluene isomers, and (d) ethyl toluene isomers on the Zr-BTB-EtOH capillary column.

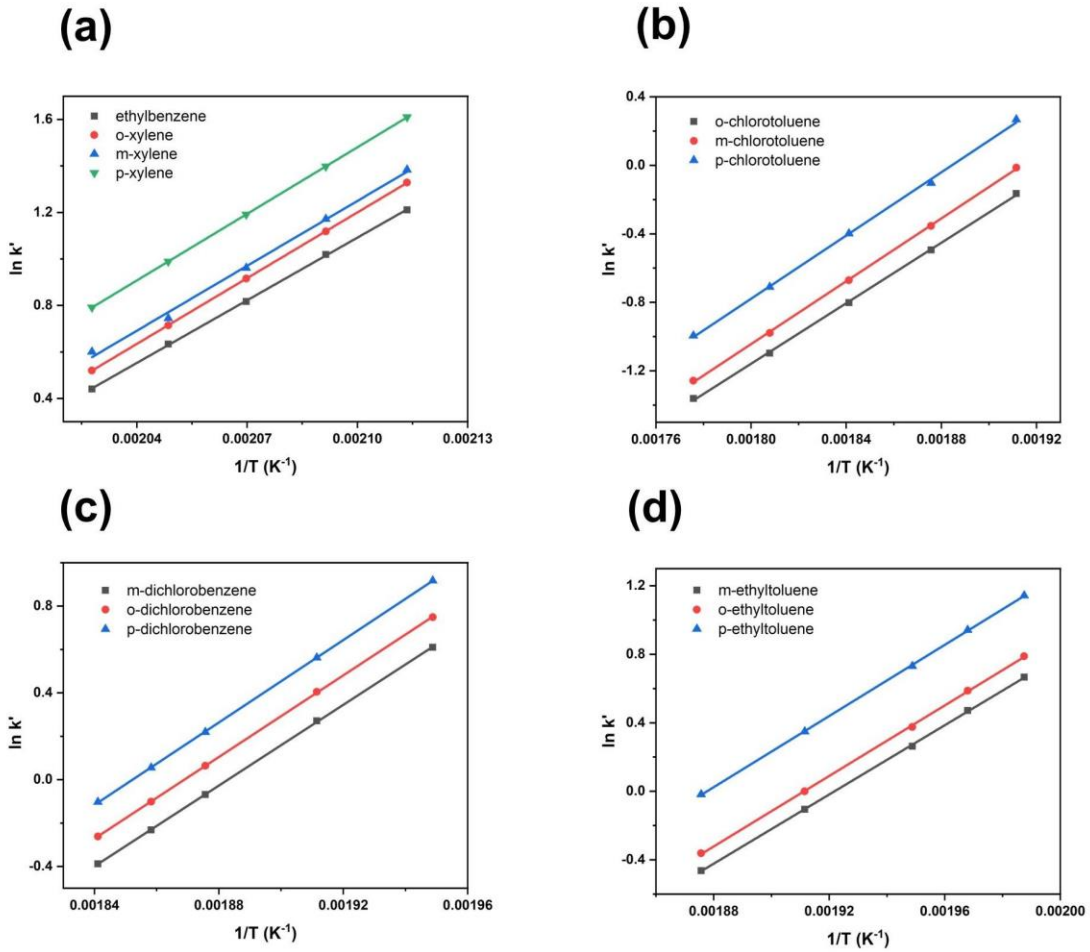

Figure S19. van't Hoff plots for (a) the xylene isomers and ethylbenzene, (b) chlorotoluene isomers, (c) dichlorotoluene isomers, and (d) ethyl toluene isomers on the Zr-BTB-PrOH capillary column.

Table S1. **Δ**H (kJ·mol^{-1}) for different isomers on the Zr-BTB coated capillary columns.

	Zr-BTB-MeOH	Zr-BTB-EtOH	Zr-BTB-PrOH
m-chlorotoluene	-84.88±2.87	-76.52±0.65	-73.39±0.8
o-chlorotoluene	-84.78±2.20	-78.66±0.58	-76.22±0.65
p-chlorotoluene	-87.18±3.36	-79.71±0.47	-76.7±1.40
m-dichlorobenzene	-76.82±0.80	-77.35±1.24	-77.33±0.36
o-dichlorobenzene	-77.39±0.81	-78.03±1.01	-78.33±0.36
p-dichlorobenzene	-78.83±0.60	-78.97±0.95	-78.96±0.25
m-ethyl toluene	-80.55±3.33	-86.34±0.71	-83.98±0.60
o-ethyl toluene	-87.03±2.55	-88.04±0.93	-85.55±0.68
p-ethyl toluene	-89.91±2.28	-88.38±0.80	-86.34±0.53
m-xylene	-80.94±4.31	-78.07±0.17	-78.36±0.10
ethyl benzene	-78.39±1.19	-78.84±1.49	-74.66±0.52
o-xylene	-80.58±4.32	-78.88±0.57	-77.35±2.60
p-xylene	-81.85±3.23	-79.63±0.06	-79.36±0.09

Table S2. ΔS ($J \cdot mol^{-1} \cdot K^{-1}$) for different isomers on the Zr-BTB coated capillary columns.

	Zr-BTB-MeOH	Zr-BTB-EtOH	Zr-BTB-PrOH
m-chlorotoluene	-136.01±34.00	-115.56±29.68	-113.32±29.93
o-chlorotoluene	-137.76±32.67	-118.39±29.51	-117.39±29.59
p-chlorotoluene	-143.67±34.92	-118.06±29.35	-116.14±30.93
m-dichlorobenzene	-117.64±30.01	-113.90±30.76	-117.14±29.10
o-dichlorobenzene	-117.65±30.01	-113.98±30.35	-117.73±28.93
p-dichlorobenzene	-118.81±29.69	-114.57±30.26	-117.89±28.85
m-ethyl toluene	-129.37±34.92	-133.94±29.76	-132.94±29.60
o-ethyl toluene	-141.17±33.34	-136.98±30.17	-135.10±29.76
p-ethyl toluene	-144.41±32.84	-133.77±30.01	-133.69±29.43
m-xylene	-132.19±35.83	-122.46±28.78	-126.21±28.69
ethyl benzene	-126.29±32.34	-123.80±31.51	-119.30±29.51
o-xylene	-131.11±37.16	-123.55±29.68	-123.63±33.84
p-xylene	-131.44±35.00	-122.88±28.06	-125.87±28.60

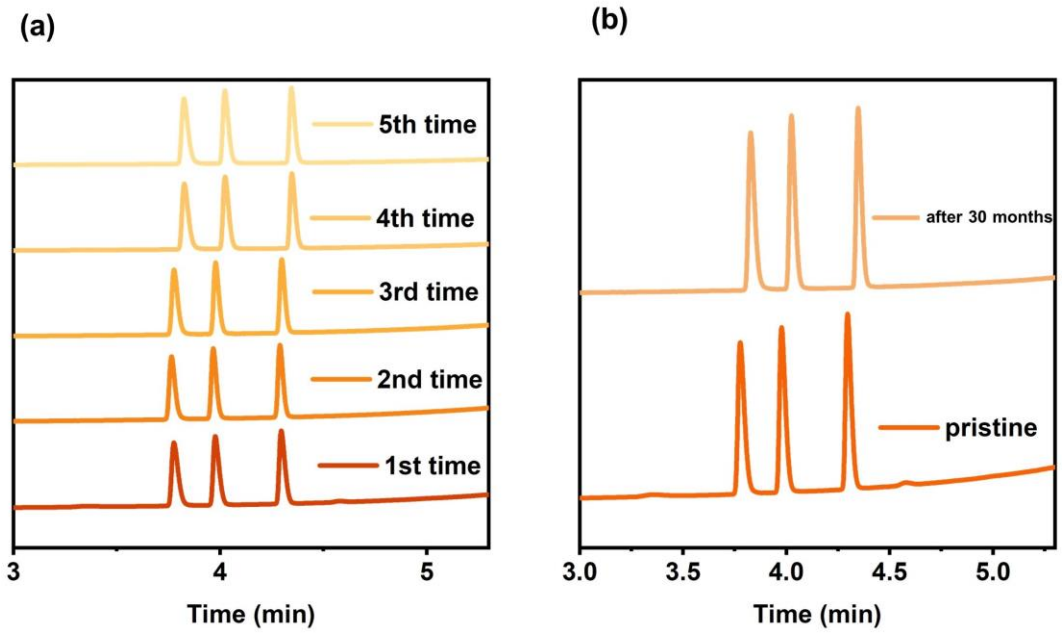

Figure S20. (a) The thermal stability and repeatability of 2-D Zr-BTB-EtOH capillary column for separation of chlorotoluene isomers 5 times continuously. (b) The lifetime of 2-D Zr-BTB-EtOH capillary column for separation of chlorotoluene isomers under the same experimental condition within 30 months.

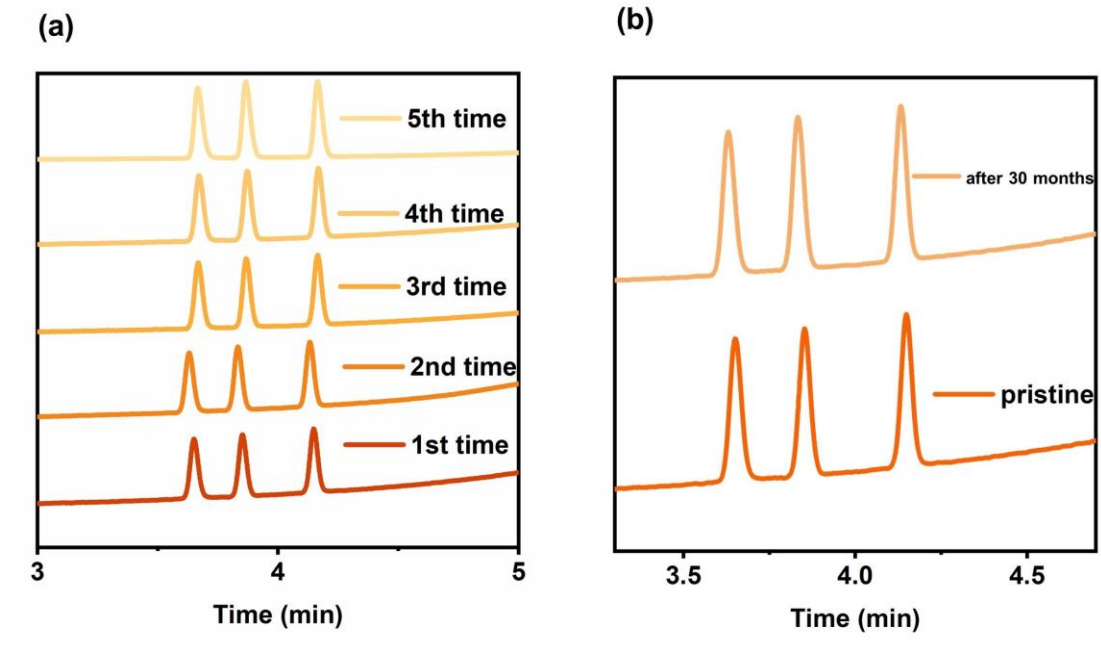

Figure S21. (a) The thermal stability and repeatability of 2-D Zr-BTB-PrOH capillary column for separation of chlorotoluene isomers 5 times continuously. (b) The lifetime of 2-D Zr-BTB-PrOH capillary column for separation of chlorotoluene isomers under the same experimental condition within 30 months.

Section S8: Characterization of Zr-TCA and Zr-TATB

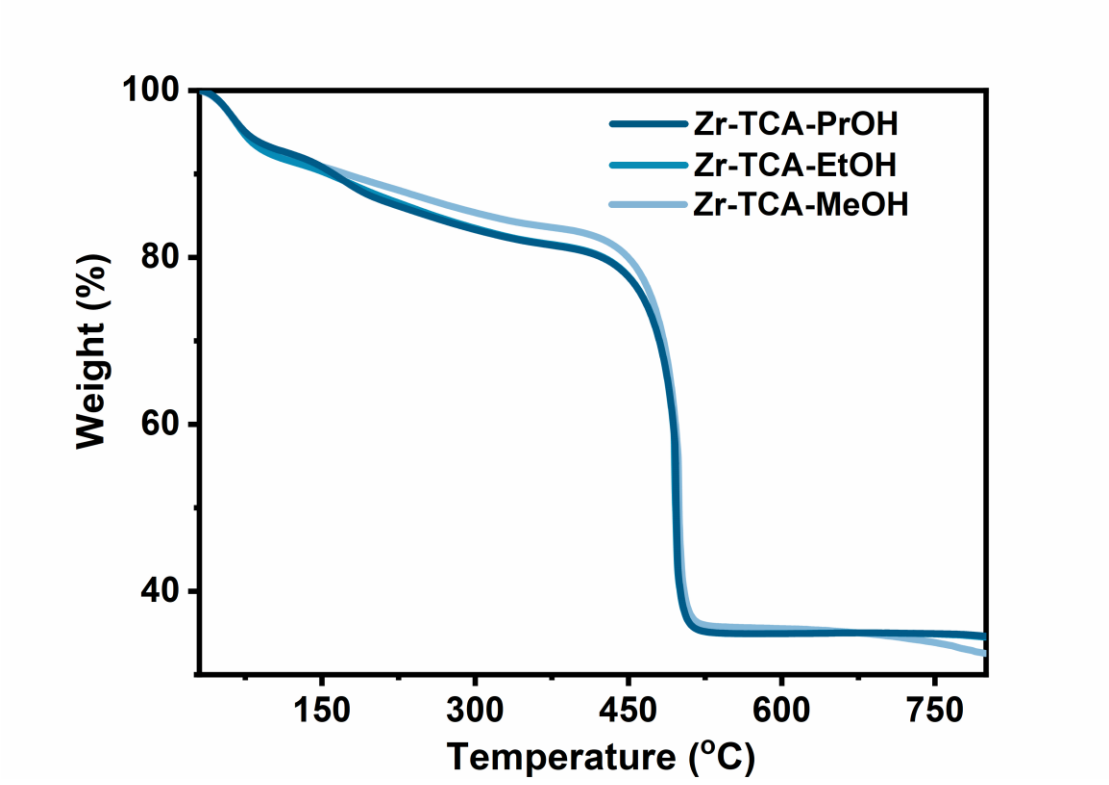

Figure S22. TGA of 2-D Zr-TCA nanosheets.

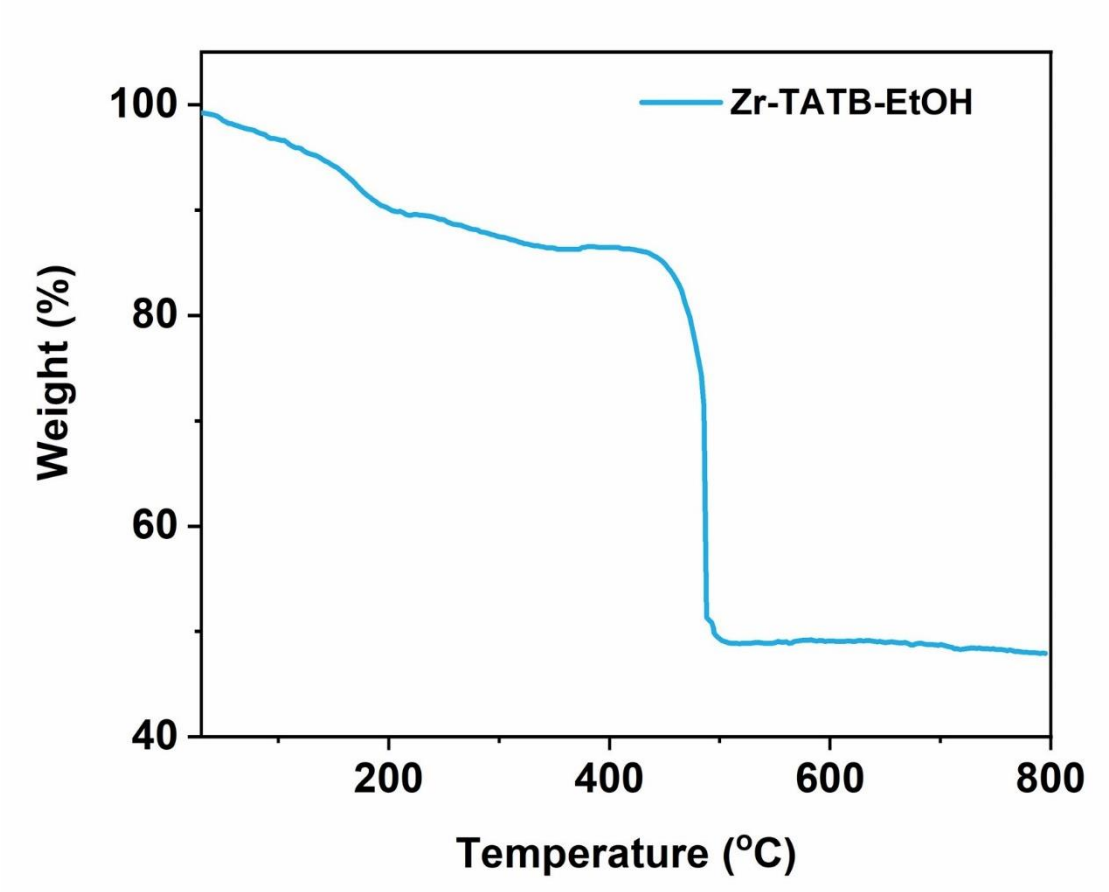

Figure S23. TGA of 2-D Zr-TATB-EtOH nanosheets.

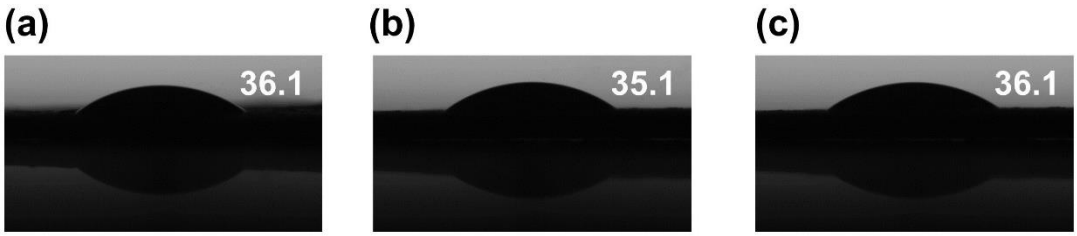

Figure S24. The water contact angle photographs of 2-D Zr-TCA-MeOH nanosheets. The water contact angle photographs were the data of the three measurements respectively. Sample preparation: the nanosheets were pressed into smooth, flat pieces.

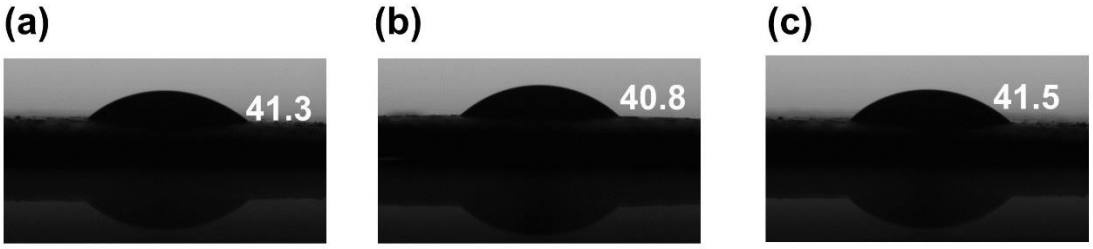

Figure S25. The water contact angle photographs of 2-D Zr-TCA-EtOH nanosheets. The water contact angle photographs were the data of the three measurements respectively. Sample preparation: the nanosheets were pressed into smooth, flat pieces.

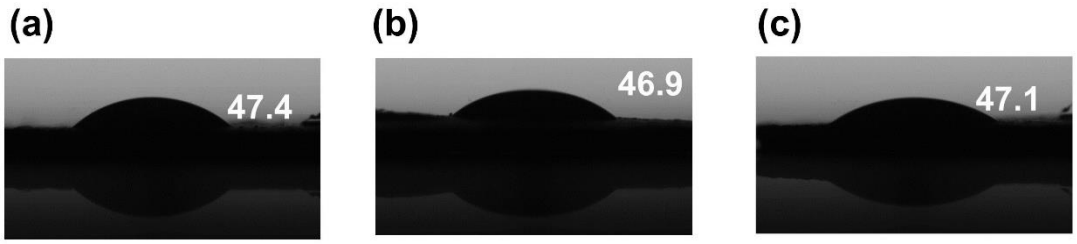

Figure S26. The water contact angle photographs of 2-D Zr-TCA-PrOH nanosheets. The water contact angle photographs were the data of the three measurements respectively. Sample preparation: the nanosheets were pressed into smooth, flat pieces.

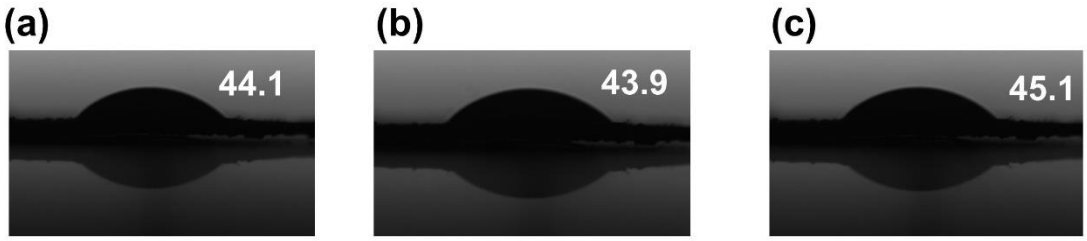

Figure S27. The water contact angle photographs of 2-D Zr-TATB-EtOH nanosheets. The water contact angle photographs were the data of the three measurements respectively. Sample preparation: the nanosheets were pressed into smooth, flat pieces.

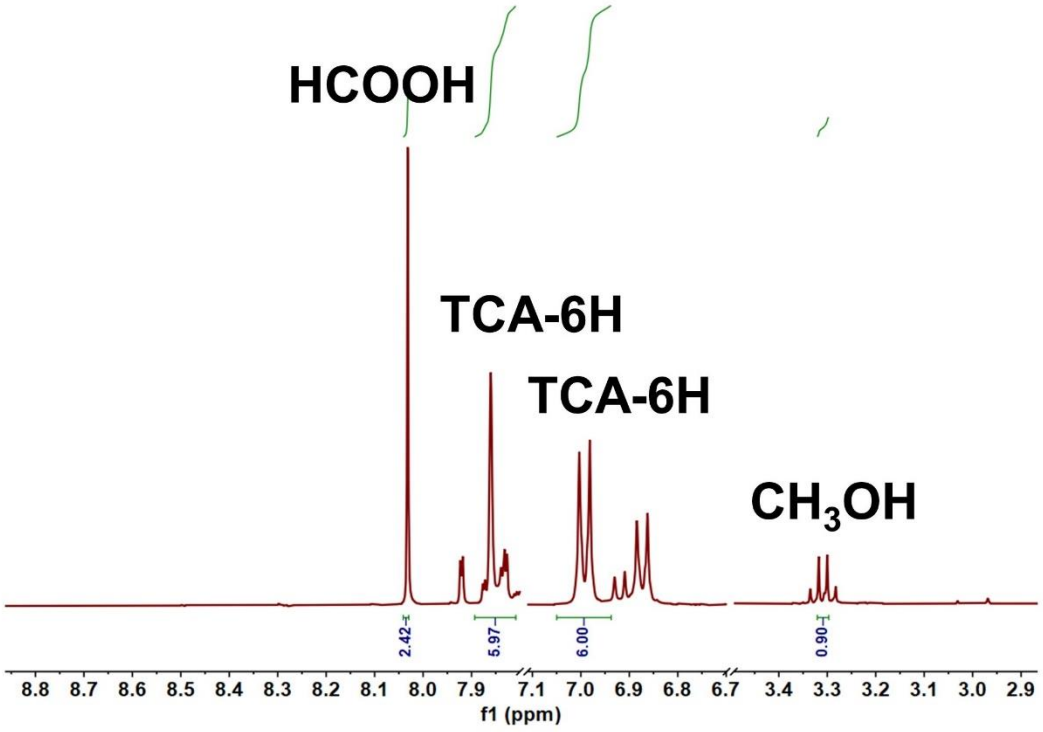

Figure S28. HNMR of 2-D Zr-TCA-MeOH nanosheets. Molar ratio of n(CH_3OH): n(BTB)=0.24: 1 was collected from the peak integration. The nanosheets sample (around 4 mg) was digested in d_6-DMSO/ K_3PO_4-D_2O (V=4:1) before HNMR measurement

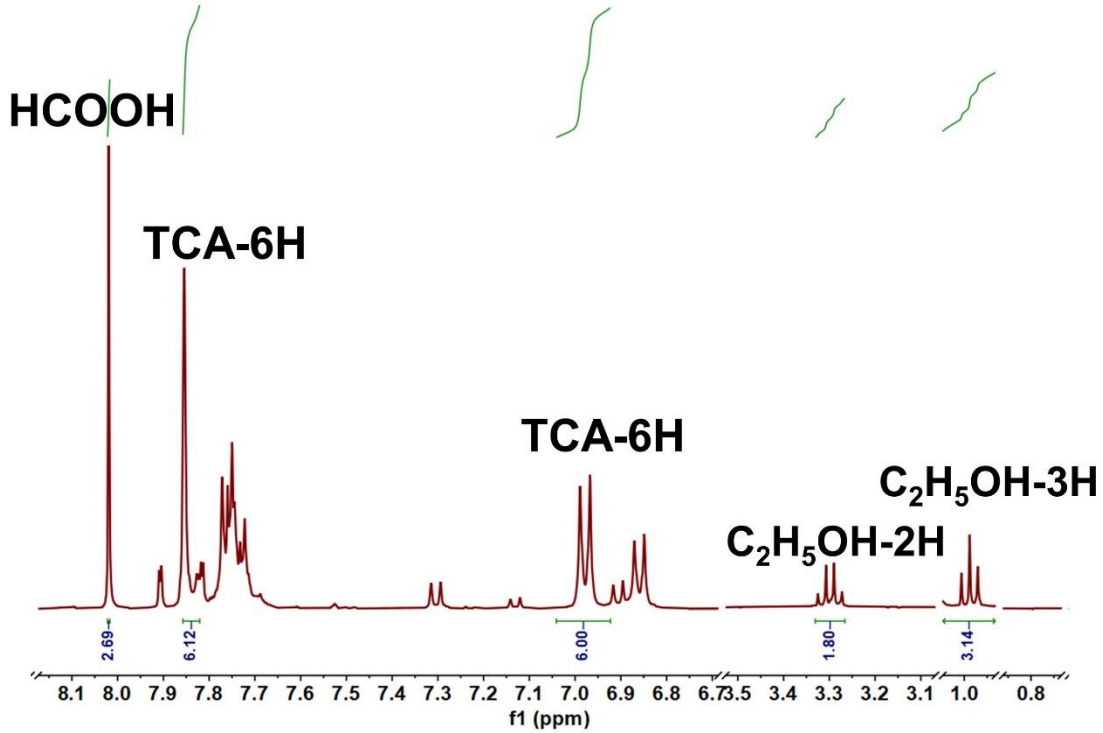

Figure S29. HNMR of 2-D Zr-TCA-EtOH nanosheets. Molar ratio of n(C_2H_5OH): n(BTB)=1.00: 1 was collected from the peak integration. The nanosheets sample (around 4 mg) was digested in d_6-DMSO/ K_3PO_4-D_2O (V=4:1) before HNMR measurement.

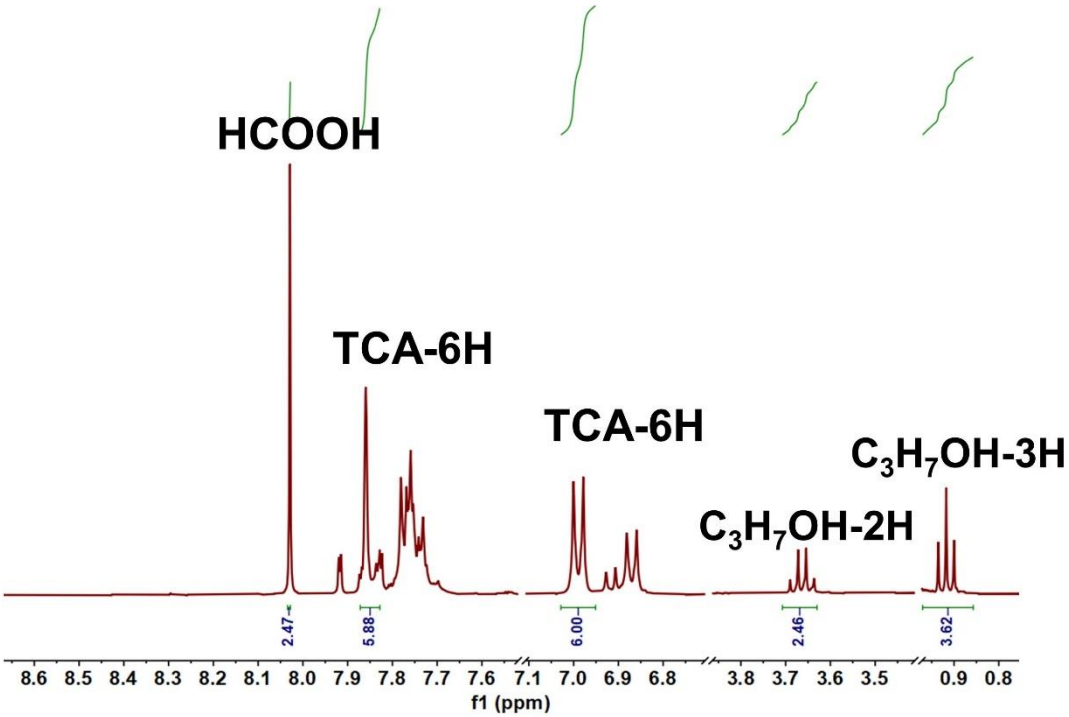

Figure S30. HNMR of 2-D Zr-TCA-PrOH nanosheets. Molar ratio of n(C_3H_7OH): n(BTB)=1.9: 1 was collected from the peak integration. The nanosheets sample (around 4 mg) was digested in d_6-DMSO/ K_3PO_4-D_2O (V=4:1) before HNMR measurement.

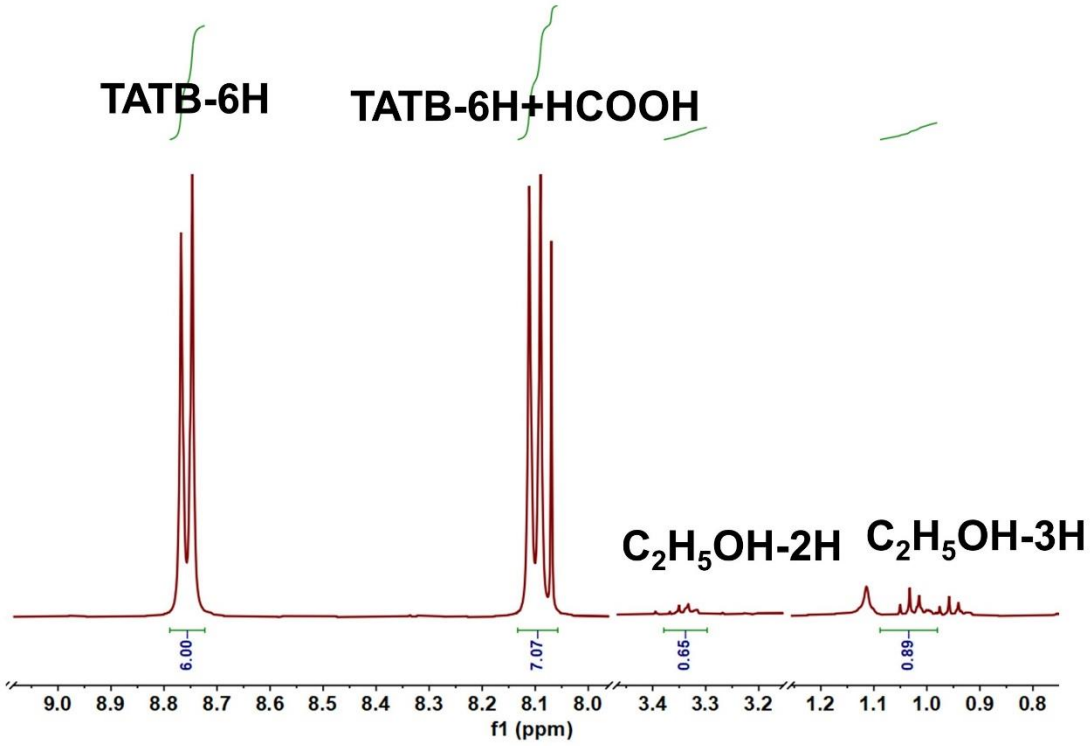

Figure S31. HNMR of 2-D Zr-TCA-EtOH nanosheets. Molar ratio of n(C_2H_5OH): n(BTB)=0.6: 1 was collected from the peak integration. The nanosheets sample (around 4 mg) was digested in d_6-DMSO/ K_3PO_4-D_2O (V=4:1) before HNMR measurement.

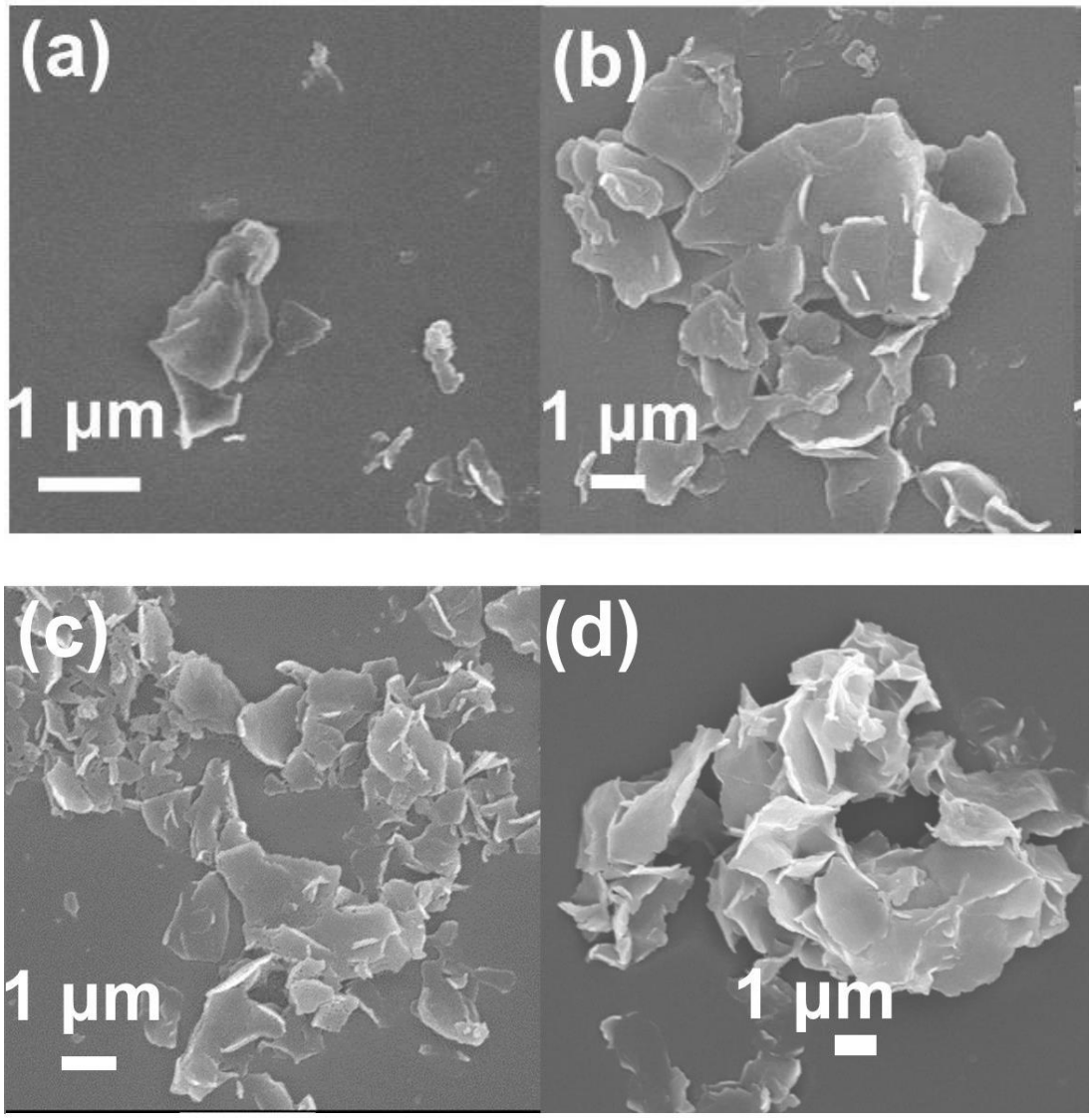

Figure S32. SEM images of (a) Zr-TCA-MeOH, (b) Zr-TCA-EtOH, (c) Zr-TCA-PrOH and (d) Zr-TATB-EtOH. The nanosheets samples were ultrasonic in methyl alcohol, ethanol and propanol solvent for 1h before TEM measurement.

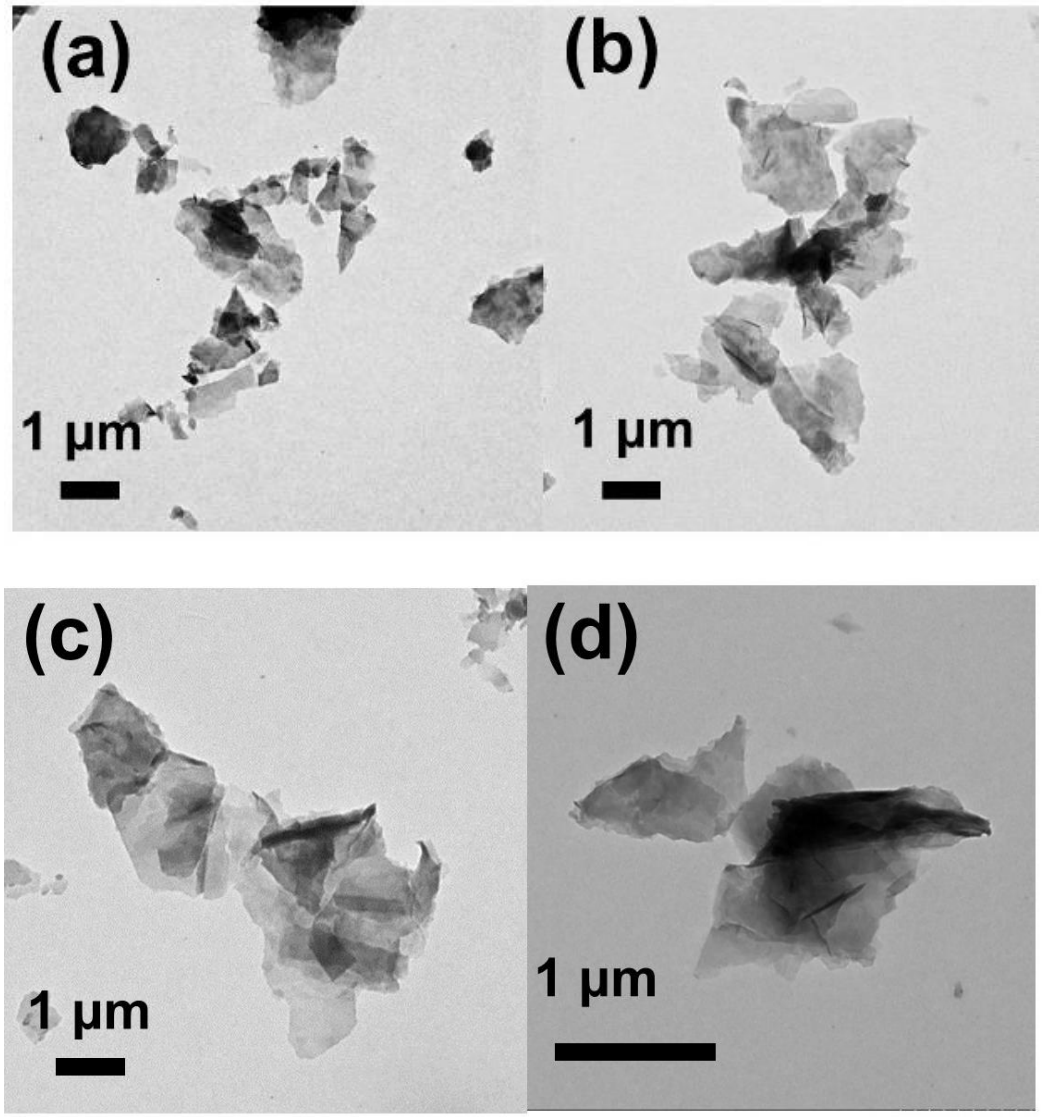

Figure S33. TEM images of (a) Zr-TCA-MeOH, (b) Zr-TCA-EtOH, (c) Zr-TCA-PrOH and (d) Zr-TATB-EtOH. The nanosheets samples were ultrasonic in methyl alcohol, ethanol and propanol solvent for 1 h before TEM measurement.

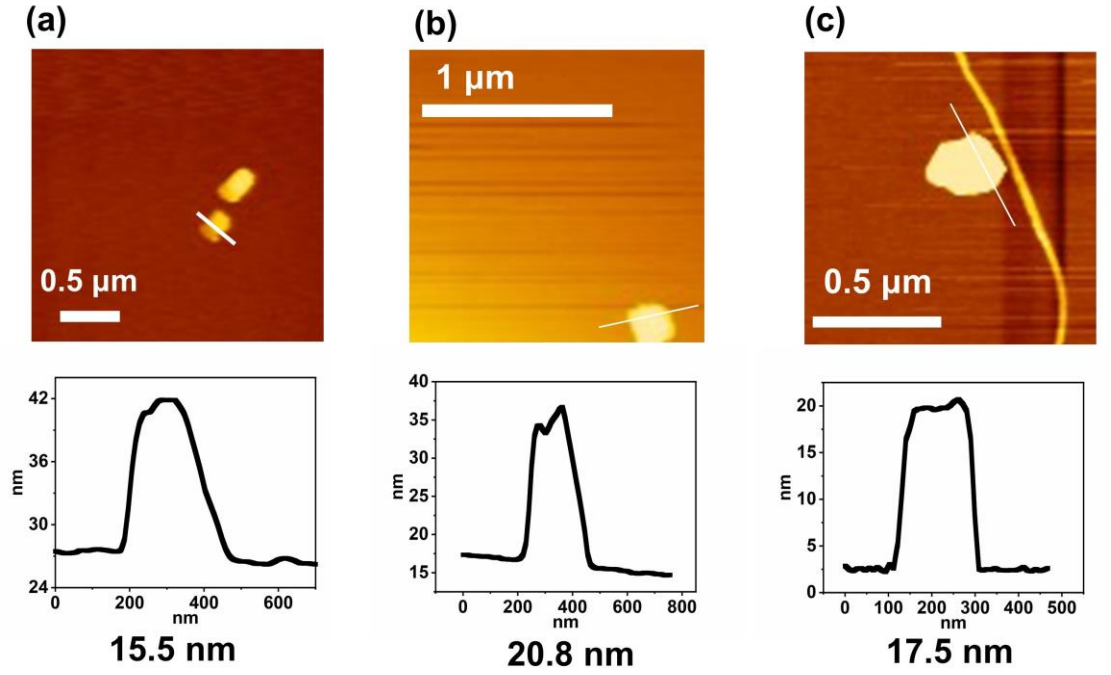

Figure S34. AFM images of synthesized Zr-TCA-MeOH nanosheets. Sample preparation: The Zr-TCA-MeOH nanosheets were dispersed into MeOH solvent and then dripped onto blank mica substrates.

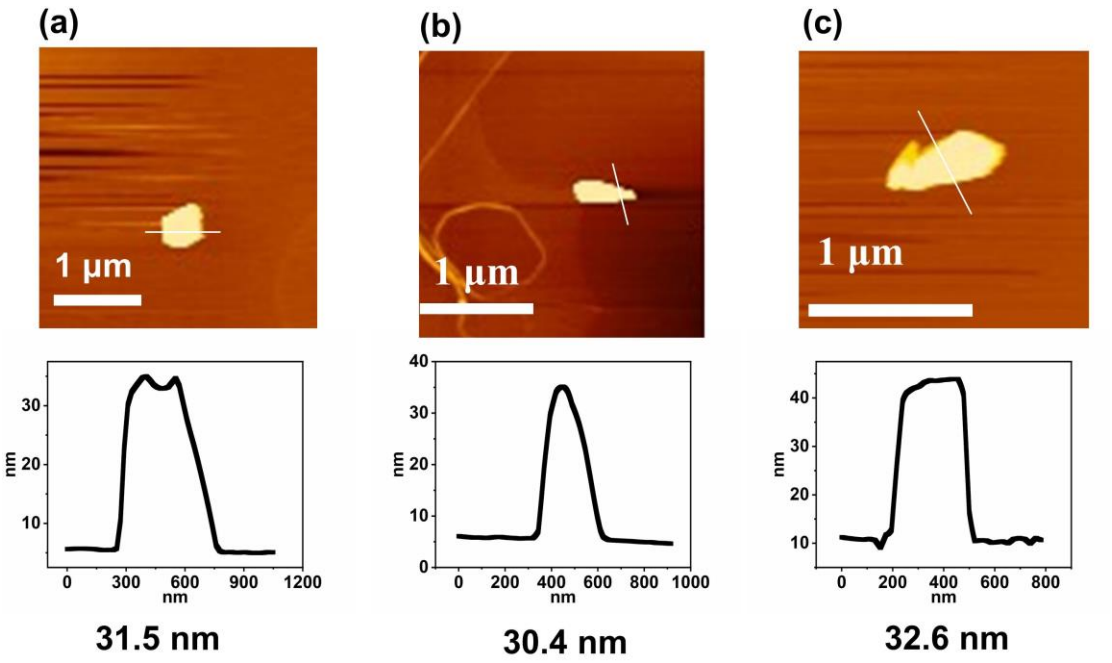

Figure S35. AFM images of synthesized Zr-TCA-EtOH nanosheets. Sample preparation: The Zr-TCA-EtOH nanosheets were dispersed into EtOH solvent and then dripped onto blank mica substrates.

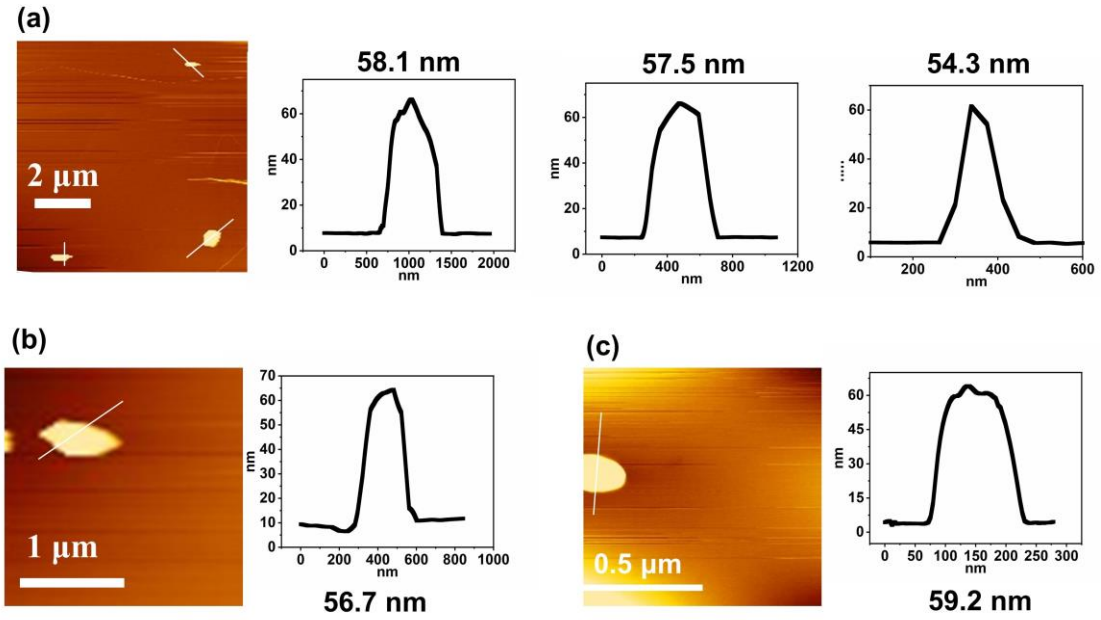

Figure S36. AFM images of synthesized Zr-TCA-PrOH nanosheets. Sample preparation: The Zr-TCA-PrOH nanosheets were dispersed into PrOH solvent and then dripped onto blank mica substrates.

Section S9: SEM Images of Zr-TCA Coated Columns and Gas Chromatogram for the Separation of Different Analytes.

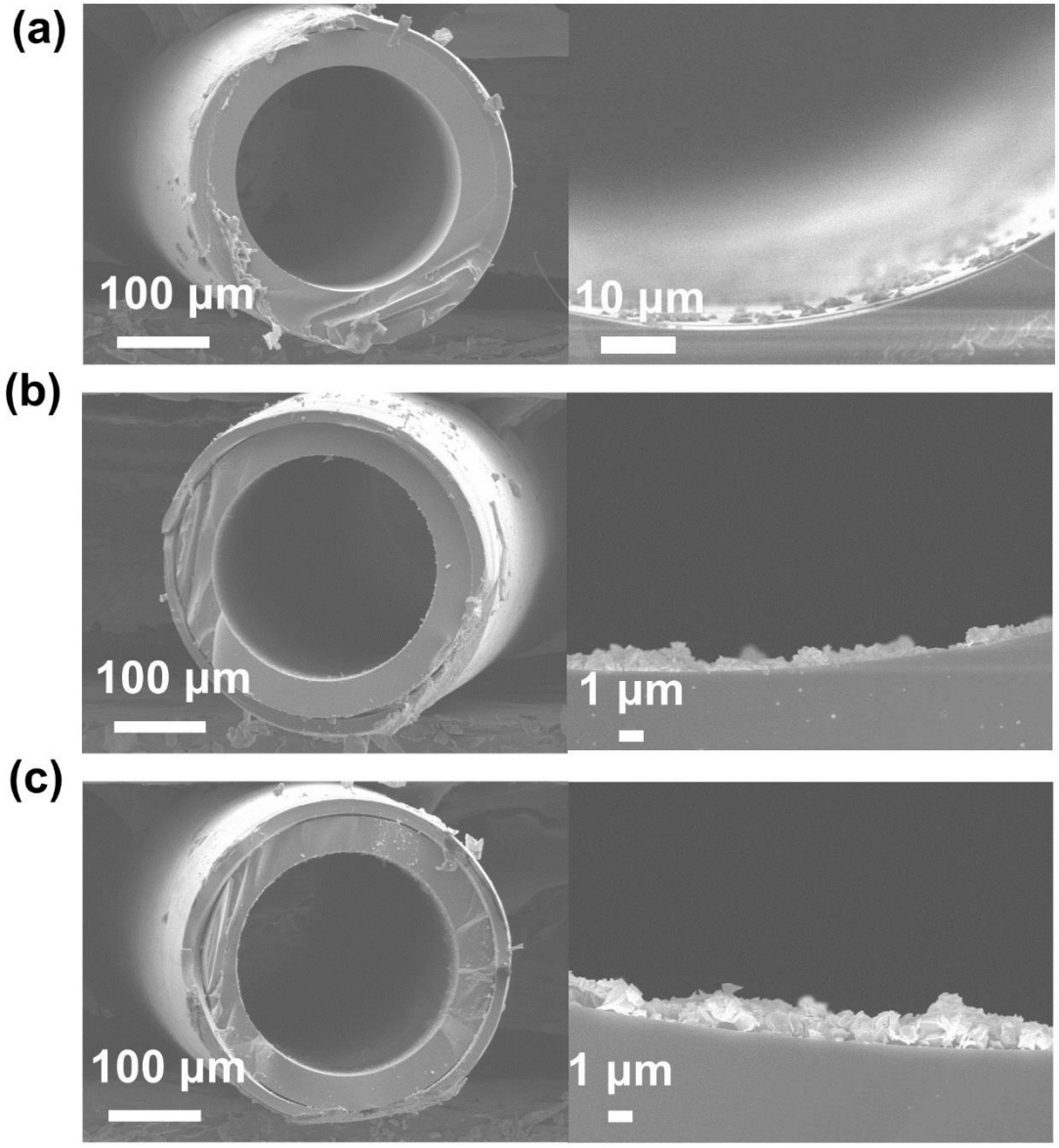

Figure S37. SEM images of (a) Zr-TCA-MeOH, (b) 2-D Zr-TCA-EtOH, and (c) 2-D Zr-TCA-PrOH capillary columns.

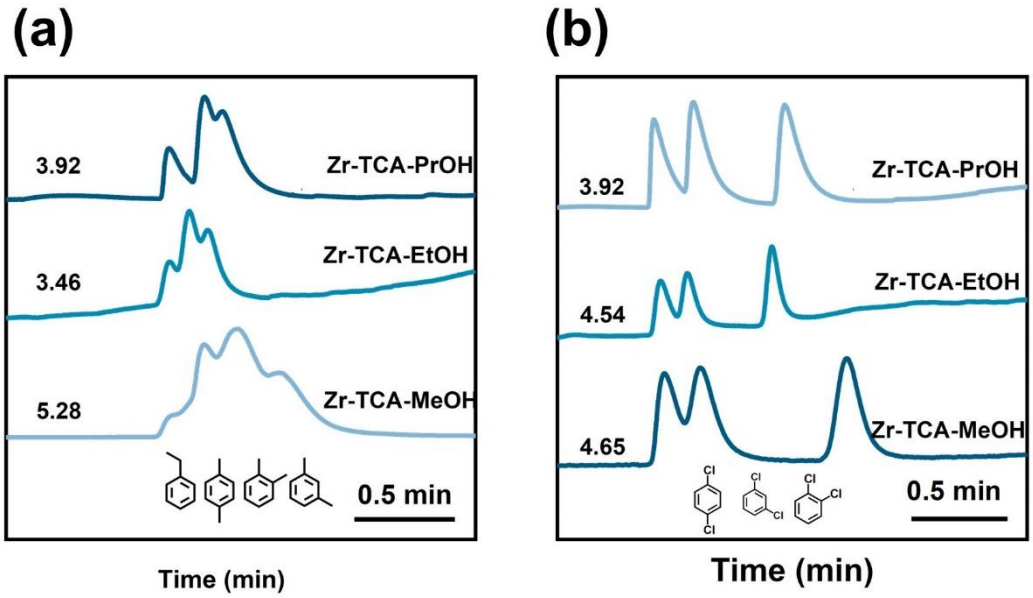

Figure S38. Gas chromatograms using 2-D Zr-TCA nanosheets coated GC columns for the separation of (a) xylene isomers and ethylbenzene and (b) dichlorobenzene isomers.

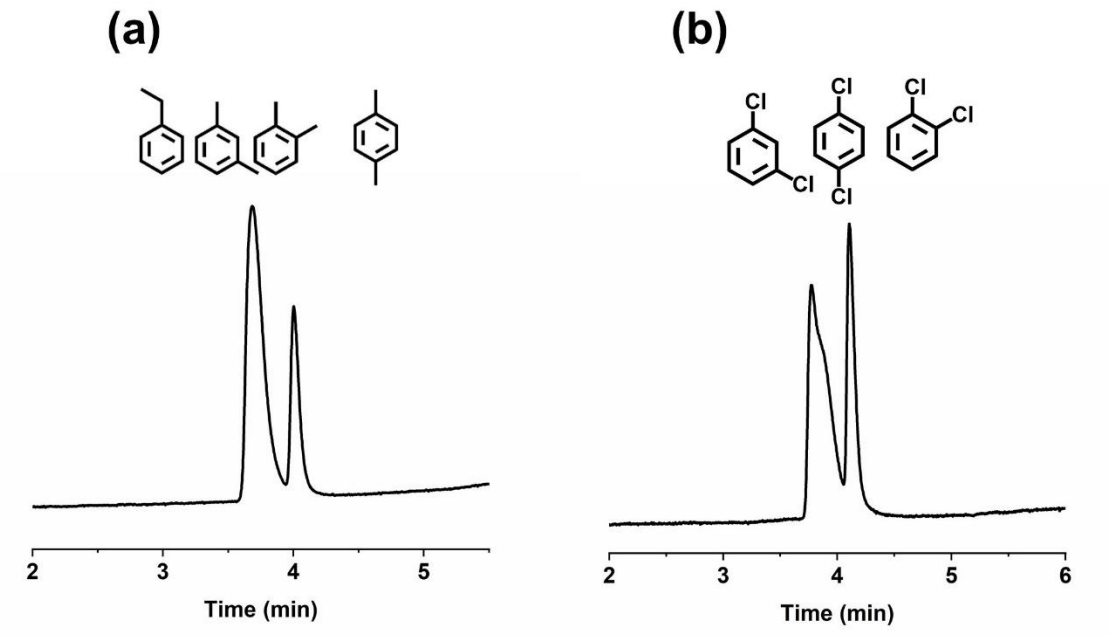

Figure S39. Gas chromatograms using 2-D Zr-TATB nanosheets coated GC columns for the separation of (a) xylene isomers and ethylbenzene and (b) dichlorobenzene isomers.

Reference

1. L. Feng, Y. Qiu, Q.-H. Guo, Z. Chen, J. S. W. Seale, K. He, H. Wu, Y. Feng, O. K. Farha, R. D. Astumian and J. F. Stoddart, *Science*, 2021, **374**, 1215–1221.
2. J. Hutter, M. Iannuzzi, F. Schiffmann and J. VandeVondele, *WIREs Comput Mol Sci*, 2014, **4**, 15–25.
3. G. Lippert, J. Hutter and M. Parrinello, *Mol. Phys.*, 1997, **92**, 477–487.
4. J. VandeVondele and J. Hutter, *J. Chem. Phys.,* 2007, **127**, 114105.
5. S. Goedecker, M. Teter and J. Hutter, *Phys. Rev. B*, 1996, **54**, 1703–1710.
6. S. Grimme, J. Antony, S. Ehrlich and H. Krieg, *J. Chem. Phys.*,2010, **132**, 154104.
7. H.-L. Qian, C.-X. Yang and X.-P. Yan, *Nat. Commun.*, 2016, **7**, 12104.